Techno-Economic Comparison of Electricity Storage Options in a Fully Renewable Energy System

Mulder, Sebastiaan; Klein, S.A.

DOI
10.3390/en17051084

Publication date
2024

Document Version
Final published version

Published in
Energies

energies

Article

Techno-Economic Comparison of Electricity Storage Options in a Fully Renewable Energy System

Sebastiaan Mulder and Sikke Klein *

Faculty of Mechanical Engineering, Delft University of Technology, 2628 CB Delft, The Netherlands; slmulder@gmx.net
* Correspondence: s.a.klein@tudelft.nl

Abstract: To support increasing renewable capacity for a net-zero future, energy storage will play a key role in maintaining grid stability. In this paper, all current and near-future energy storage technologies are compared for three different scenarios: (1) fixed electricity buy-in price, (2) market-based electricity buy-in price, and (3) energy storage integrated into a fully renewable electricity system. In the first part of this study, an algorithm is devised to simulate strategic buy-in of electricity for energy storage. This analysis yields a qualitative decision-making tool for a given energy storage duration and size. Building upon the first part's findings, an integration study gives insight into expected power prices and expected storage size in a typical northwestern European fully renewable energy system. The integration study shows significant need for electricity storage with durations spanning from one to several days, typically around 40 h. Pumped Hydro Storage and Pumped Thermal storage surface as the best options. The overall levelized costs of storage are expected to be in the USD 200–500/MWh range. Integration of storage with renewables can yield a system-levelized cost of electricity of about USD 150/MWh. Allowing flexibility in demand may lower the overall system-levelized cost of electricity to USD 100/MWh.

Keywords: batteries; energy storage; grid stability; LCOE; markets; modelling; net-zero

check for updates

Citation: Mulder, S.; Klein, S. Techno-Economic Comparison of Electricity Storage Options in a Fully Renewable Energy System. *Energies* **2024**, *17*, 1084. https://doi.org/10.3390/en17051084

Academic Editor: Marco Merlo

Received: 9 January 2024
Revised: 18 February 2024
Accepted: 20 February 2024
Published: 24 February 2024

1. Introduction

Given the substantial growth in variable renewable power generation in recent years, with expectations of further increases, the issue of grid stability is progressively becoming a more pressing concern. Energy storage is widely regarded as one of the key enablers of a future energy system with a high share of variable renewable power generation [1,2]. Historically, there was little need for energy storage systems due to widely available dispatchable electricity generation. While technologically, electricity storage is feasible, the cost level compared to the dispatchable fossil fuel alternative has prohibited large-scale deployment [3]. In recent years, interest in energy storage has increased as a method to mitigate volatility induced by the rapid increase in variable renewable electricity generation in the energy system.

Despite the important role of cost in energy storage, it proves difficult to equally compare energy storage technologies. This is often the case due to the varying definitions of levelized cost of storage (LCOS), different discharge durations or number of yearly discharges, or different assumptions made. In recent years, excellent technology reviews on energy storage have been published, most notably by the Storage Lab led by Oliver Schmidt [4,5]. This study aims to further clarify the comparison of the various available energy storage technologies by including the effect of a time-varying power price, including more energy storage technologies, such as Pumped Thermal Energy Storage, and including the analysis of electricity storage in a fully renewable power system. In the context of this paper, three main metrics of power price are used: $LCOE_{storage}$ represents the overall levelized cost of electricity coming from energy storage systems, including the energy buy-in price. $LCOE_{generation}$ refers only to the renewable power generation cost, without storage.

$LCOE_{system}$ represents the levelized cost of electricity for the whole system, consisting of renewable generation, electricity storage, and backup power.

This paper starts with a general introduction of the LCOS methodology as developed by Schmidt [6] and a comprehensive description of the thirteen electricity storage technologies considered in this study. In the first part of this paper, the storage technology options are economically compared for different applications using the methodology developed by Schmidt [6]. The main parameters distinguishing storage options are the number of cycles per year, the average duration of release of power, the round-trip efficiency, the costs for the intake of electricity, and the investment costs. With these parameters, different storage technology options will be compared based on the levelized cost of energy storage, $LCOE_{storage}$.

In the second part of this paper, the identified electricity storage options are included in a balance model that describes a "zero-dimensional" electricity grid, assuming no restrictions in electricity transport between supply, demand, and storage. The time-dependent behavior of the electricity grid is modelled using public data for electricity consumption in Germany, in combination with public data for electricity generation in Germany from solar PV and offshore wind (data for the years 2020–2023). The balance in the grid model is realized through a combination of assumed flexibility in demand, energy storage, and backup power. Several optimization studies have been performed to determine the most economically attractive combination for different combinations of parameters.

A comprehensive overview of the structure of this paper is given in Figure 1.

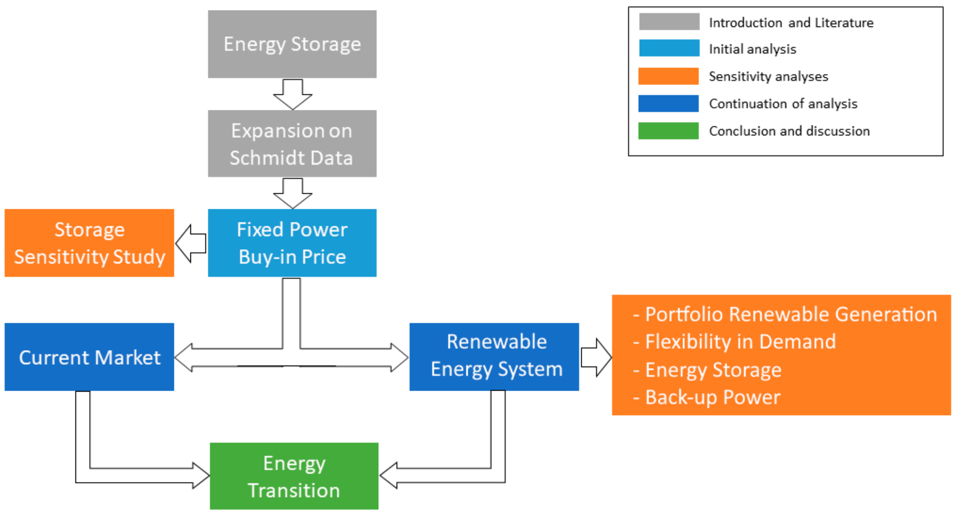

Figure 1. Diagram of the structure of this paper.

2. Materials and Methods

2.1. LCOS Methodology

To compare energy storage technologies in this paper, the levelized cost of storage (LCOS) methodology of Schmidt [5] is used, which calculates the total discounted $LCOE_{storage}$ of stored energy based on capital expenditure (CAPEX), operational expenditure (OPEX), charging cost, end-of-life cost, and the total discharged capacity in the technology's lifetime. $LCOE_{storage}$ is thus the sum of all costs divided by the sum of all energy discharged. In the remainder of this paper, $LCOE_{storage}$ is used to indicate the levelized cost of electricity of stored energy, including charging cost. $LCOE_{storage}$ is calculated as [5]:

$$LCOE_{storage} = \frac{C_{CAPEX} + \sum_{n}^{N} \frac{C_{OPEX}}{(1+r)^n} + \sum_{n}^{N} \frac{C_{charge}}{(1+r)^n} + \frac{C_{EoL}}{(1+r)^{N+1}}}{\sum_{n}^{N} \frac{E_{discharged}}{(1+r)^n}}. \tag{1}$$

This model assumes capital investment cost is incurred at the beginning of construction and sums up all discounted costs every year (n) up to the system's financial lifetime (N), discounted by the given discount rate (r). Yearly costs, such as maintenance, or non-yearly costs, such as replacements, are incurred in their respective years. In the model, it is also assumed that energy storage always goes through a full cycle, meaning that it is charged until completely full and discharged until completely empty; the size of this full cycle is determined by the capacity and the depth of discharge of the respective technologies. This will result in the lowest possible storage cost, as the largest amount of energy is discharged from the storage. To match market demand, it may often be more beneficial to not fully discharge or charge the storage; however, this will lead to increased storage cost per unit of energy discharged, as there will be less energy stored in the storage over its lifetime. The effect of the latter is further investigated in the second part of this paper.

The total discharged capacity is calculated as follows [5]:

$$\sum_{n}^{N} \frac{E_{discharged}}{(1+r)^{n}} = Y_{cycles} \cdot DoD \cdot E_{cap} \cdot \eta_{RT} \cdot \left(1-\eta_{self}\right) \cdot \sum_{n=1}^{N} \frac{\left(1-D_{cyc}\right)^{(n-1)Y_{cycles}} \cdot \left(1-D_{t}\right)^{(n-1)}}{(1+r)^{n+t_{c}}}. \quad (2)$$

Here, Y_{cycles} is the number of cycles per year, DoD is the depth of discharge, E_{cap} is the energy capacity, n_{RT} is the round-trip efficiency, n_{self} is the self-discharge per cycle, t_c is the construction time in years, D_{cyc} is the cyclical degradation, and D_t is the annual degradation.

2.1.1. Capital Expenditure (C_{CAPEX})

The investment costs are the result of the capital cost per unit of power, the capital cost per unit of capacity, and the replacement cost. Replacement cost is defined as costs incurred due to major replacements over the life cycle of the storage. These replacements are incurred only in the year they occur and therefore differ from general yearly operation and maintenance (O&M) costs. Capital expenditure is calculated as follows [5]:

$$C_{CAPEX} = C_{p} \cdot P_{cap} + C_{e} \cdot E_{cap} + \sum\nolimits_{m=1}^{M} \frac{C_{p-r} P_{cap}}{(1+r)^{t_{c}+m+t_{r}}}. \quad (3)$$

Here, C_p is the cost per unit of power, P_{cap} is the rated power, C_e is the cost per unit of capacity, E_{cap} is the rated capacity, M is the number of replacements needed in the system's lifetime, $C_{P\text{-}r}$ is the replacement cost per unit of power, m is the current replacement, and t_r is the time interval of replacements.

2.1.2. Operations and Maintenance (C_{OPEX})

OPEX accounts for maintenance and operation costs and is calculated as [5]:

$$\sum\nolimits_{n}^{N} \frac{C_{OPEX}}{(1+r)^{n}} = \sum\nolimits_{n}^{N} \frac{C_{p-OM} P_{cap} + C_{e-OM} \cdot \left(Y_{cycles} \cdot DoD \cdot E_{cap}\right) \cdot \left(1-D_{cyc}\right)^{(n-1)Y_{cycles}} \cdot \left(1-D_{t}\right)^{(n-1)}}{(1+r)^{n+t_{c}}}. \quad (4)$$

Here, $C_{p\text{-}OM}$ is the (operations and maintenance) O&M cost per unit of power, $C_{e\text{-}OM}$ is the O&M cost per unit of capacity, D_{cyc} is the degradation per cycle, and D_t is the annual degradation.

End-of-Life (C_{EOL})

End-of life costs include reclamation of parts and decommissioning costs, and they are calculated as [5]:

$$\frac{C_{EoL}}{(1+r)^{N+1}} = \frac{EoL_{p} \cdot P_{cap} + EoL_{e} \cdot E_{cap}}{(1+r)^{N+1}}. \quad (5)$$

Here, EoL_p is the end-of-life cost per unit of power and EoL_e the cost related to end-of-life per unit of capacity. Note that the end-of-life cost might increase if the technology is to be repurposed, such as for lithium-ion batteries [6].

2.1.3. Charging Costs (C_{charge})

Different scenarios for charging costs can be applied. In this paper, first, a fixed cost per MWh is assumed. In the second analysis, market prices are used for charging costs.

2.2. Description of Energy Storage Technologies

This study aims to incorporate all energy storage technologies that are currently already in use or are expected to be ready for deployment in the near future. To this end, thirteen different energy storage technologies are considered. Here, simplifications are made in the categorization of the technologies, as the average values of each technology are taken. Results for specific variations of the various categories may vary slightly. The aim of this study is therefore to identify trends and make generic conclusions. In this section, a short introduction to each technology and the accompanying assumptions are given, including the source of the data presented. For new technologies, an indication of the technology readiness level (TRL) is given, which gives insight into the distance from commercial deployment. The information is derived from several papers and reports, including the most recent publications of the International Energy Agency on this subject [7].

2.2.1. Lithium-Ion Battery (Li-Ion)

Lithium-ion batteries account for most of the newly installed energy storage capacity, with 16 GW installed as of 2021 [8]. This technology is already relatively mature, even for grid-scale application, as there are already some projects up to 600 MW/2400 MWh in use today, and larger ones are being planned [9]. Popularized through their use in electric vehicles, Li-ion batteries have experienced a large price drop in recent years. Although during the COVID-19 pandemic the price rose due to difficulties in the supply chain for raw materials, a general downward trend in price is predicted until approximately 2040 [10]. Disadvantages of this technology are fire hazard, short lifespan, limited depth-of-discharge (+/−80%), price for long-term storage, ethical issues with mining of various metals, such as lithium, and the predicted scarcity and price increase of lithium. Recycling of lithium is currently limited and expected to cost up to USD 20/kWh of capacity installed [5,6]. Repurposing lithium-ion batteries currently results in a higher $LCOE_{storage}$ than recycling; therefore, prices may go up in the future [6]. On the other hand, as lithium-ion batteries have a high learning rate, prices of Li-ion batteries may also drop in the future [11,12]. As the future price of Li-ion batteries is unclear, in this analysis, the current value of 2023 is taken. The effect of a potential future price drop is evaluated in a sensitivity analysis in this paper.

2.2.2. Sodium–Sulfur Battery (NaS)

Steady-state sodium–sulfur batteries were first developed by NGK Insulators and Tokyo Electric Power about 35 years ago [13]. These batteries have a relatively long lifetime and need little precious metals. The battery must be kept at an elevated temperature upwards of 300 degrees Celsius to keep the materials liquified. Uncontrolled cooling down of the battery will lead to significant damage. As capacity can be scaled up well, this technology is generally capable of capacities slightly larger than Li-ion batteries [14]. Several projects are operational, leading to a TRL of 8 [7].

2.2.3. Lead–Acid Battery (LeadAcid)

Lead–acid batteries can be found in cars, but they also serve a minor role in energy storage. The technology is relatively low in capital cost and easy to implement. The disadvantages are the low round-trip efficiency (RTE), short lifespan, and rapid degradation. This solution is generally recommended only for very irregular use [15].

2.2.4. Vanadium Flow Battery (VaFlow)

The vanadium flow battery is a type of flow battery better suited to long-term storage. The electrolytes are stored in separate tanks. The advantage of flow batteries is that capacity (MW) and storage volume (MWh) can easily be separated. The vanadium flow battery is considered in this study as the most advanced type of flow battery, with a relatively high TRL. The vanadium flow battery has a longer lifetime than lithium-ion batteries and a reduced fire risk [16]. Current challenges for vanadium flow batteries include relatively low power and energy density. Various other types of flow batteries exist, with the most prominent being vanadium and zinc-based flow batteries [17]. New flow batteries are being researched, such as aqueous flow batteries [17]. The vanadium flow battery has a TRL of 8, and some full-scale installations are operational in the world [7].

2.2.5. Rankine-Type Thermal Energy Storage (RTES)

Rankine-Type Thermal Energy Storage is a thermal energy storage technology that generally makes use of resistive heaters to charge the system and a Rankine cycle to discharge the system. This technology can, in principle, be retrofitted in any steam Rankine cycle if the steam parameters of the turbine are matched. To-be-decommissioned coal-fired power plants can thereby be transformed into energy storage plants, thus retaining their workforce, site utilities, and saving expenses on the turbomachinery [18]. For the cost estimation in this model, the turbomachinery is therefore assumed to be free. There will still be a cost associated with power due to the electric heaters, piping, and auxiliary equipment. This energy storage category may sometimes be referred to as electrical thermal energy storage (ETES); in this paper, the term RTES is coined to differentiate this technology from other forms of ETES that do not make use of a Rankine cycle and therefore cannot be retrofitted into a coal-fired power plant [19].

As RTES makes use of a steam turbine, start-up flexibility is limited, and a cold start after more than 60 h of standstill can take up to 3 h. Hot start-up is considerably faster [20].

The costs of RTES are based on an engineering best guess, which reflects prices stated by commercial developers; the power-scaled cost of RTES technology is approximated according to the cost of an industrial e-boiler multiplied by 5 to account for higher pressure, engineering cost, EPC cost, additional piping, and a larger pressure vessel [21]. The capacity-scaled cost is approximated as the capacity-scaled cost of PTES, scaled to match the lower thermal efficiency.

There is a limited number of RTES small-scale demonstration plants in the world; however, this technology has never been applied at a large scale. High-temperature heat storage has a typical TRL of 7–8, and the combination with a Rankine cycle will result in a TRL of around 6 [7].

2.2.6. Pumped Thermal Energy Storage (PTES)

Pumped Thermal Energy Storage, otherwise known as the Brayton Battery, is a relatively old concept for energy storage, but it has had a resurgence in recent years. This storage technology makes use of hot and cold reservoirs, such as crushed rock or molten salt for the hot reservoir and hexane for the cold reservoir. A theoretical maximum efficiency of up to 72% is reported for the technology depending on the temperature differential between hot and cold storage and the thermodynamic efficiencies of the equipment [22]. More realistically, efficiencies between 52 and 58% are expected [19,23]. Storage capacity in MWh of PTES is relatively cheap and expandable independent of power; therefore, the technology is more geared towards long-term storage. Implementations vary, but the hot reservoir is generally heated to 550–600 °C in commercial applications, so there is the possibility of heat and power cogeneration. The disadvantage of this high temperature is the energy loss. There are several companies working on commercialization of this concept, but large-scale facilities are not yet in use. The TRL is below 6 [7].

As there is still a large range of uncertainty within the concept, a conservative estimate of the costs is taken. Maintenance cost is estimated to be equal to aCAES [23].

2.2.7. Pumped Hydro Storage (PHS)

Pumped Hydro Storage is a highly efficient and widely used method of energy storage that has been used since the 1890s [24]. It operates on a simple yet ingenious principle: excess electricity is used to pump water from a lower reservoir to an upper reservoir during periods of low electricity demand. To recover the potential energy, the stored water is released from the upper reservoir to the lower one. As it flows down, it passes through a turbine, generating electricity to be fed back into the grid.

Most PHS systems around the world are in the range of 1000–1500 MW, with some up to 3000 MW. The typical round-trip efficiency of PHS systems is around the 70–80% range [24]. The technology is very mature, but, surprisingly, it displays a negative learning rate, meaning that the technology is getting more expensive as more is built [5]. An important reason behind this is that many suitable locations for PHS systems are already in use.

2.2.8. Compressed Air Energy Storage (aCAES and dCAES-H2)

Compressed Air Energy Storage (CAES) technology stores energy through the compression of air. The temperature increase from the compression can either be stored in thermal storage or discharged to the environment via cooling. Cooling down of the high-pressure air before storage is required to reduce storage size, complexity, and heat losses during storage. The high-pressure air from the storage must be heated up to increase the output and to prevent extremely low temperatures before expansion in a turbine. The technology is either called adiabatic CAES (aCAES) in cases where the compression heat is stored and reused or diabatic CAES (dCAES) in cases where external heat is used to preheat the high-pressure air before expansion.

As compressed air is assumed to be stored in a salt cavern, this technology is geographically limited.

While no commercial aCAES plants have been built yet, two large-scale dCAES projects are in commercial operation. For aCAES, only some small-scale demonstrators are operational, and the TRL is therefore below 7 [7].

The dCAES using natural gas has a TRL of 9. The TRL of dCAES using hydrogen is mainly dependent on the hydrogen combustion system. This technology has a TRL of around 7 for gas turbine technology.

As there are no financial numbers available for aCAES installations, the CAPEX for aCAES is based on dCAES numbers in which the thermal storage is assumed to be 25% of the CAPEX [4,25,26]. The costs of the dCAES-H2 technology are modelled as a superposition of hydrogen electrolyzer and hydrogen storage costs in addition to the conventional dCAES storage costs. The future hydrogen electrolyzer cost is estimated to be USD 880/kW. For reference, current electrolyzer costs are about USD 1500/kWh, and optimistic estimates go as low as USD 400/kW for 2030 [4,27,28].

2.2.9. Liquid Air Energy Storage (LAES)

Liquid Air Energy Storage uses thermal cycles like PTES to store energy in the form of both liquid air and heat in cold and hot reservoirs. The cold reservoirs operate at cryogenic temperatures. The different implementations of LAES vary widely in costs and round-trip efficiency, and the largest variations are due to the efficiency of the usage of the stored heat and cold. LAES is available in a diabatic and an adiabatic form. Diabatic LAES requires reheating of the air, conventionally performed with natural gas. In this study, only adiabatic LAES is considered. Cost values are extrapolated from a techno-economic evaluation of a 60 MW, 480 MWh case [29]. The round-trip efficiency is taken as the mean of reported round-trip efficiencies across various studies. The maintenance cost is estimated to be equal to aCAES [29–31].

2.2.10. Hydrogen Gas Turbine (H2-CCGT)

Direct combustion of hydrogen in a combined-cycle gas turbine installation can provide a carbon-neutral and flexible storage solution while profiting from the maturity of the gas turbine industry [32,33]. However, while great efforts have been made in advancing the hydrogen readiness of gas turbines, the availability and cost of hydrogen are still a major bottleneck [34].

The cost of the combined-cycle gas turbine is approximated as the cost of a conventional CCGT at USD 797/kWh; this is deemed reasonable but slightly optimistic, as other sources report higher values and a hydrogen combustion system is needed [4,32]. The cost of the electrolyzer is taken as the moderate value for 2030, equal to USD 880/kWh [4]. Combustion of hydrogen in a combined-cycle gas turbine installation has an increased efficiency over a simple-cycle gas turbine, at the expense of some start-up flexibility. The steam turbine in a CCGT is the main bottleneck for start-up, and it may take up to 2–3 h to start up during a cold start, which is typically after more than 60 h of standstill. Starting a CCGT after less than 60 h of standstill is considerably faster, and modern CCGT power plants require less than 30 min from start signal to full load [20]. A certain amount of energy is lost during start-up. This leads to reduced efficiency; therefore, an LHV efficiency of 58% is used instead of the typical 60% for a modern CCGT.

The TRL of hydrogen application in gas turbines is 7 [7].

2.2.11. Hydrogen Gas Turbine Retrofit (H2-CCGT-R)

Instead of constructing an entirely new gas turbine, it may be possible to retrofit a hydrogen burner in an existing gas turbine. This technology is currently in development and is expected to be ready for deployment before electrolyzer capacity catches up to speed [33]. This option is attractive for gas turbines relatively close to a salt cavern suited for hydrogen storage, as it dramatically cuts down on capital expenditure versus a new power plant. In this paper, the cost of this retrofit is assumed to be 10% of the CAPEX of a new gas turbine combined-cycle installation.

2.2.12. Hydrogen Fuel Cell (H2-FuelCell)

Instead of a gas turbine, a fuel cell may also be used to convert hydrogen to electricity. Fuel cells are generally used for smaller applications. Storage of the hydrogen is assumed to be in a salt cavern because of its low cost. Fuel cells are more flexible for start-up than CCGTs. Moderate 2030 values are taken for the cost values. The thermal efficiency of a fuel cell is assumed to be 50%, which is slightly lower than a combined-cycle gas turbine installation (58%) [5,32].

2.3. Data Input to the Model

All data inputs to the model for the various energy storage technologies can be found in Table 1.

Table 1. Data used for cost calculation of energy storage technologies. Main sources are indicated with superscript: a = [5], b = [23], c = [31], d = [4], and e = [32]. Cited values have been cross-checked with [4,6,10,13,22,27,32,34,35]. Values without a source are the best estimate. All values should be interpreted as moderate future values around 2030. Assumptions are given in the paragraphs above.

	Li-Ion	**NaS**	**LeadAcid**	**VaFlow**	**PTES**	**aLAES**	**RTES**	**PHS**	**aCAES**	**dCAES-H2**	**H2-CCGT**	**H2-CCGT-R**	**H2-FuelCell**
CAPEX (USD/kW)	250 [a]	650 [a]	300 [a]	700 [a]	797 [b]	2000 [c]	300	1100 [a]	980 [d]	1230 [d]	1600 [d]	980 [d]	2050 [e]
CAPEX (USD/kWh)	300 [a]	450 [a]	320 [a]	450 [a]	21 [b]	500 [c]	63	50 [a]	30 [d]	3 [d,e]	3 [d,e]	3 [d,e]	3 [d,e]

Table 1. *Cont.*

	Li-Ion	NaS	LeadAcid	VaFlow	PTES	aLAES	RTES	PHS	aCAES	dCAES-H2	H2-CCGT	H2-CCGT-R	H2-FuelCell
CAPEX Factor (-)	1	1	1	1	1	1	1	1	1.25 [d]	1	1	1	1
OPEX (USD/MWh)	0.4 [a]	0.4 [a]	0.4 [a]	2 [a]	2.6 [d]	2.6 [d]	2.6 [d]	0.4 [a]	2.6 [d]	3.3 [d]	3 [d]	3 [d]	3 [d]
OPEX (USD/kW-y)	5 [a]	5 [a]	5 [a]	10 [a]	11 [d]	11 [d]	11 [d]	11 [d]	11 [d]	14.9 [d]	3.2 [e]	3.2	28.5 [e]
Replacement (USD/kW)	50 [a]	-	-	90 [a]	-	-	-	120 [a]	100 [a]	100 [a]	-	-	-
Replacement (USD/kWh)	150 [a]	-	-	0 [a]	-	-	-	0 [a]	0 [a]	0 [a]	-	-	-
Rep. Interval (10^3)	3.5 [a]	-	-	3.5 [a]	-	-	-	7.3 [a]	1.5 [a]	1.5 [a]	-	-	-
EoL (USD/kW)	0 [a]	20 [a]	20 [a]	20 [a]	20 [a]	20 [a]	20 [a]	20 [a]	20 [a]	20 [a]	20 [a]	20 [a]	20 [a]
EoL (USD/kWh)	20 [a]	0 [a]	0 [a]	−100 [a]	0 [a]	0 [a]	0 [a]	0 [a]	0 [a]	0 [a]	0 [a]	0 [a]	0 [a]
RTE (-)	86% [a]	75% [a]	72% [a]	68% [a]	57.5% [b]	49.3% [c]	41.8%	80% [a]	70% [d]	55% [d]	41% [d]	41% [d]	35% [e]
DoD (-)	80% [a]	80% [a]	80% [a]	100% [a]	100%	100%	100%	100% [a]	100% [a]	63% [d]	63% [d]	63% [d]	63% [d]
Self-Discharge (1/c)	1% [a]	5% [a]	1% [a]	-	2% [b]	1% [b]	2% [b]	-	0.75% [d]	0% [d]	0% [d]	0% [d]	0% [d]
Cycle Life (10^3 cycles)	3.5 [a]	4 [a]	0.9 [a]	20 [a]	14.6 [b]	10 [a]	10 [a]	30 [a]	15 [a]	15 [a]	10 [a]	10 [a]	10 [a]
Shelf Life (y)	20	15 [a]	10 [a]	20 [a]	20 [b]	20 [d]	30 [d]	80 [d]	35 [d]	35 [d]	30 [d]	30 [d]	30 [e]
Degradation (1/y)	1% [a]	1% [a]	1% [a]	0.15% [a]	-	-	-	-	-	-	-	-	-
End-of-Life (-)	80% [a]	80% [a]	80% [a]	95% [a]	80%	95%	95%	95% [a]	95% [a]	95% [a]	95% [a]	95% [a]	95% [a]
Construction Time (y)	1 [a]	1 [a]	1 [a]	1 [a]	1	1	1	3 [a]	2 [a]	2 [a]	2 [a]	2 [a]	1

2.4. Geographical Restrictions

Depending on local circumstances, not all energy storage technologies may be possible. To this end, six different scenarios are evaluated in this paper, as given in Table 2. Here, greenfield means no geographical features and no retrofit options available; therefore, PHS, CAES, hydrogen storage, and all retrofit options are not possible. If a cavern feature is present, all greenfield options plus CAES and hydrogen options are possible. The mountains scenario allows for all greenfield options plus PHS. Coal retrofit allows for all greenfield options plus RTES, and lastly, gas retrofit together with a cavern allows for all greenfield options, all cavern options, and hydrogen-fired CCGT retrofit. Finally, all options are included in the scenario "all options".

Table 2. Applicability of the different energy technologies in the different scenarios.

	Li-ion	**NaS**	**LeadAcid**	**VaFlow**	**PTES**	**aLAES**	**RTES**	**PHS**	**aCAES**	**dCAES-H2**	**H2-CCGT**	**H2-CCGT-R**	**H2-FuelCell**
All options													
Greenfield													
Cavern													
Mountains													
Coal retrofit													
Gas retrofit													

2.5. Part I: Comparison of Storage Technologies Using the Levelized Cost of Storage Methodology

In this first part of this paper, several methodologies are compared to calculate the levelized costs of storage for the different storage technologies. The main objective of these analyses is to distinguish the most economically favorable technologies; the technologies will be ranked for different storage applications, and the overall $LCOE_{storage}$ will be calculated.

2.5.1. Fixed-Price Charging Cost Analysis

Different charging costs have been studied. In the first analysis, charging costs are taken as constant USD 100/MWh and USD 50/MWh, and USD 100/MWh reflects a typical, approximate, current median wholesale power price [36]. In the second analysis, a market-based charging price has been studied. This market-based charging price is calculated using a novel algorithm: the retrospective lowest possible charging price algorithm (RLPCP). This algorithm is applied to the Day-Ahead prices in Germany in 2023.

To evaluate the robustness of the ranking of the different technologies, the sensitivity of the ranking of the technologies depending on the CAPEX development has been studied in a separate sensitivity study, found in the discussion.

2.5.2. Charging of the Storage Based upon Market Power Prices

Previous studies have often assumed a constant power price for charging [5]. In recent years, the market power price has been more volatile than ever; therefore, energy storage technologies may profit from a cheaper price if periods of low or negative power price are leveraged. In this study, an algorithm is devised that gives the Retrospective Lowest Possible Charging Price (RLPCP).

The algorithm in this study serves as an approximation of the real charging power price and gives an estimate of the minimum possible charging tariff using historical price data.

In the model, part-load or partially charging or discharging is neglected. It is assumed that the storage is charged and discharged at the same power, limited by the electrical connection. Charging will therefore be slower than discharging, as energy is lost during storage. The energy lost in the storage is given by the round-trip efficiency. The factor with which charging takes longer than discharging is thus given by the reciprocal of the round-trip efficiency (RTE). As the discharge will always be at full power in this model, discharging time ($t_{discharge}$) equals the ratio between capacity and power, also called the E/P ratio (EP). The charging time is then calculated by:

$$t_{charge} = \frac{t_{discharge}}{RTE} = \frac{EP}{RTE} \tag{6}$$

The time domain is a discrete series containing price data. A moving average filter with the size t_{charge} is applied to the time domain; this will yield the moving average domain. The moving average domain will have a length of t_{charge} shorter than the time domain. The minimum of the moving average domain will equal the average lowest price when the storage is charged during a continuous period of duration t_{charge}.

If the number of yearly cycles is more than one, a second minimum needs to be found. This time, part of the time domain is already occupied by the first cycle because it is not possible to charge twice during the same timeslot. Figure 2 gives a schematic overview of this algorithm. In Figure 2, the part of the time series reserved for charging is given in blue. The green cell of the moving average domain indicates the found minimum of the moving average domain. The three cells reserved for charging in the time domain can be translated to the moving average domain as $t_{charge} - 1$ cells left and right of the found minimum. These cells are indicated in red. All cells that are not yet "reserved" in the moving average domain can still be utilized. For the next iteration, the blue cells that are occupied for charging and the purple cells that are reserved for a possible discharge will be appended to the list of reserved cells in the time domain.

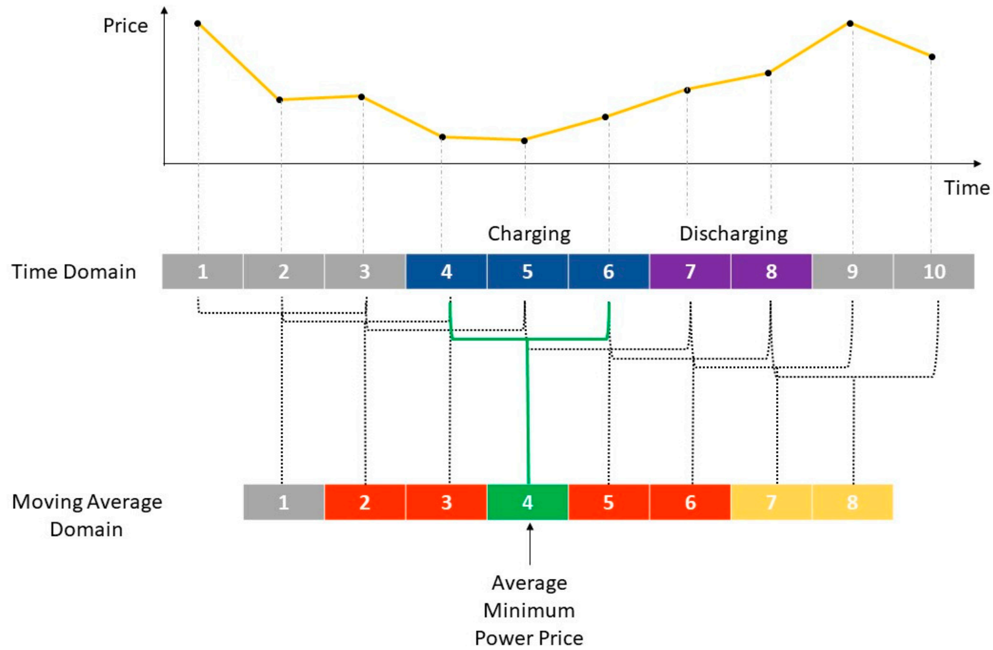

Figure 2. Visualization of the RLPCP algorithm, here with a charging duration of 3 and a discharging duration of 2, both unitless for convenience.

Lastly, it is not possible for storage to consecutively load twice without discharging. Therefore, the absolute minimal amount of time after which the storage can be charged again equals a duration of $t_{charge} + t_{discharge} = CD_{factor}(1 + EP)$ after first starting charging. This is given as purple cells in the time domain and translates to the yellow cells in the moving average domain. These timesteps are therefore reserved for one cycle. Note that as discharging profits are not considered, discharge does not need to happen in the allocated discharging time; this can be anywhere between the completion of charging and the start of the charge of the next cycle. As the cycle always starts at a low price point followed by a higher price point, it is assumed that a suitable discharge time can be found, thus giving an estimate of the minimum possible buy-in price for the given number of cycles. As the number of cycles increases, the power buy-in price approaches the average power price over the year, but it will always stay under the average price over the year.

Figure 3 shows an example of the algorithm at work for $t_{charge} = 3$ and $t_{discharge} = 2$ over the course of 3 days for better visibility. In Figure 3, 3 cycles occur, and the average power buy-in price is given below the charging period. The light-colored areas in the moving average domain give the total reserved space in the moving average domain. The dark-colored areas in the time domain indicate the chosen charging periods. Figure 4 displays one week in which the maximum number of cycles is achieved. The RLPCP algorithm numbers the charging intervals based on the order of realized charging prices during the individual intervals.

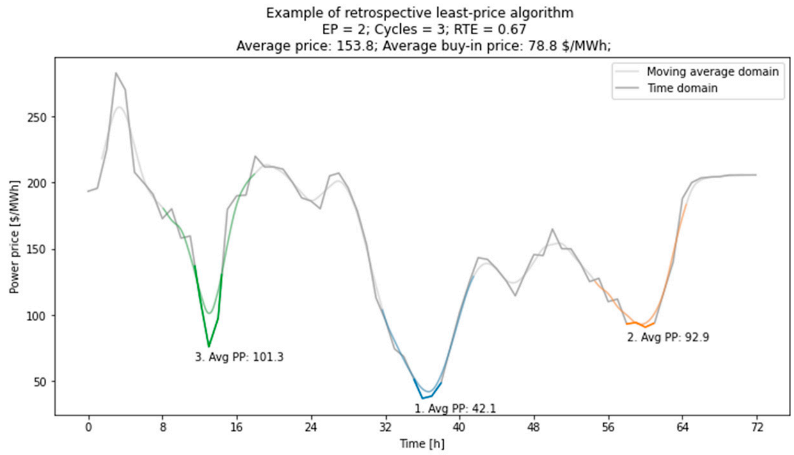

Figure 3. Example of the RLPCP algorithm selecting the cheapest intervals for charging over 3 days, colors indicate the charging intervals.

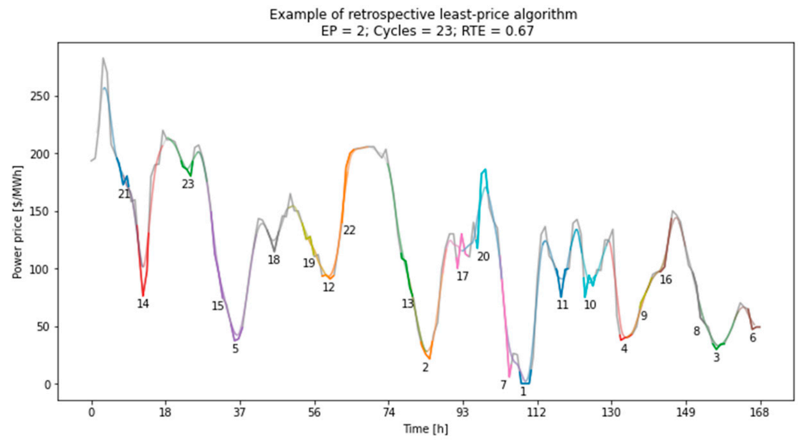

Figure 4. Example of the RLPCP algorithm selecting the cheapest intervals for charging during one week of operation, colors indicate the charging intervals.

2.6. Part II: Energy Storage in a Fully Renewable Electricity System

The optimal energy storage solution as part of a fully renewable energy system depends on many factors. In this paper, the impact of the most relevant factors is studied using a zero-dimensional, time-dependent electricity balance model. It is called a zero-dimensional (0D) grid as no limitations in electricity transport over the grid are considered. The main parameters in this zero-dimensional electricity balance model, shown in Figure 5, are:

- The generation of renewable electricity through solar PV and offshore wind.
- Demand, including flexibility in demand.
- Energy storage, as described in the first part of this paper.
- Backup power.

Backup power is introduced to guarantee an overall balance between demand and supply at all moments. Backup power is therefore defined at any moment t as:

$$P_{backup}(t) = P_{renewable}(t) + P_{storage}(t) - P_{demand}(t) \tag{7}$$

It is assumed in this analysis that there is always enough backup power. An important aspect of backup power is that the energy for the backup power is not generated by the renewable electricity sources within the system but is supplied from outside of the system.

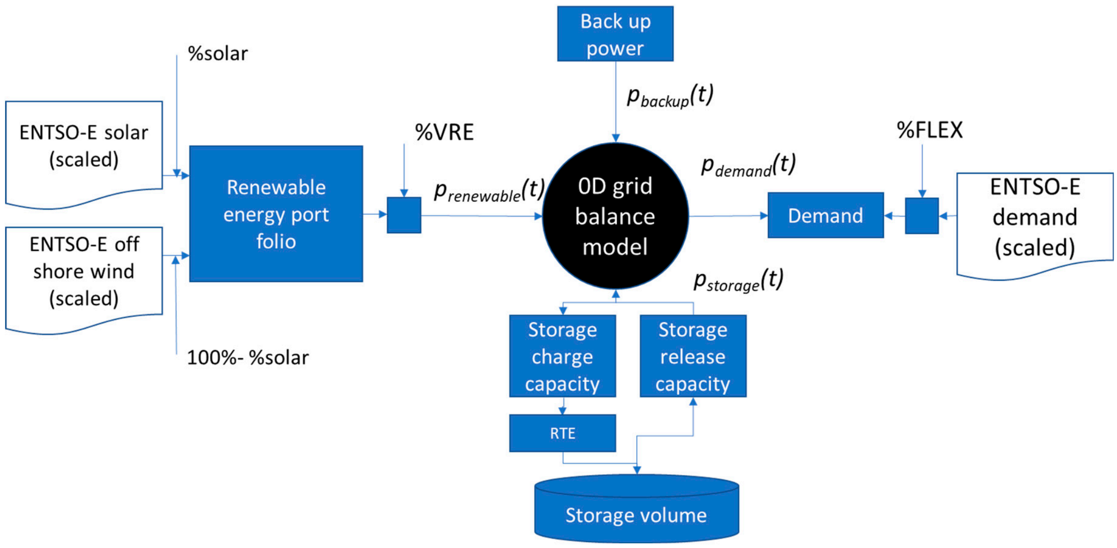

Figure 5. The system studied. The grid is fed by a virtual renewable energy portfolio consisting of offshore wind and solar. The profiles of offshore wind, solar, and demand are based on ENTSO-E data for Germany. The backup energy is only used during moments of a shortage of wind and solar energy and energy from storage.

In a real-world system, backup power could be provided by thermal power plants running on fossil fuels. These fossil fuels can be replaced by carbon-neutral fuels in the future, like hydrogen, generated outside of this system.

In the model, it is further assumed that the excess of renewable generation will be curtailed.

The profiles of yearly solar PV and offshore wind electricity production as well as demand are taken from the ENTSO-E website for Germany for the years 2020–2023. The ENTSO-E Transparency Platform is regarded as the most prominent energy data source for European energy systems [37,38]. The solar PV capacity profile, offshore wind capacity profile, and demand profile from ENTSO-E have been scaled to their annual average values. The analyses deliver similar results for all years from 2020 to 2023. The year 2023 has been chosen as input for the shown analyses.

Two main renewable energy sources are considered in this system analysis: offshore wind and solar PV. These technologies are expected to be among the dominant energy sources in energy systems in 2050 [39,40]. On-shore wind has been excluded from the portfolio as it appeared to have only a limited effect on the annual duration curve of the renewable electricity supply.

2.6.1. Portfolio of Renewable Generation

The levelized costs of electricity of the total system will be lowest when the energy profile provided by the renewable portfolio matches demand as close as possible. In this high-level analysis, a constant baseload demand is assumed, but similar conclusions can be drawn for a realistic demand. Figure 6 presents an analysis of this optimization. The annual duration curves for 100% German solar electricity generation, provided by ENTSO-E, are compared to those of 100% offshore wind. The annual duration curves have been scaled to have identical numbers for annual MWh generated and consumed. In these annual duration curves, the generation per hour is sorted from the largest to the smallest.

These annual duration curves show that offshore wind is much closer to baseload demand than solar PV. Solar can only provide the required demand for 2800 h; during the other hours, there is a shortage in electricity that must be delivered by another source, such as backup power. For solar, this would be about 60% of the annual demand. For offshore wind, the situation is much better, as can be seen in the top-right figure. The total annual shortage in electricity generation is about 30% of the annual demand.

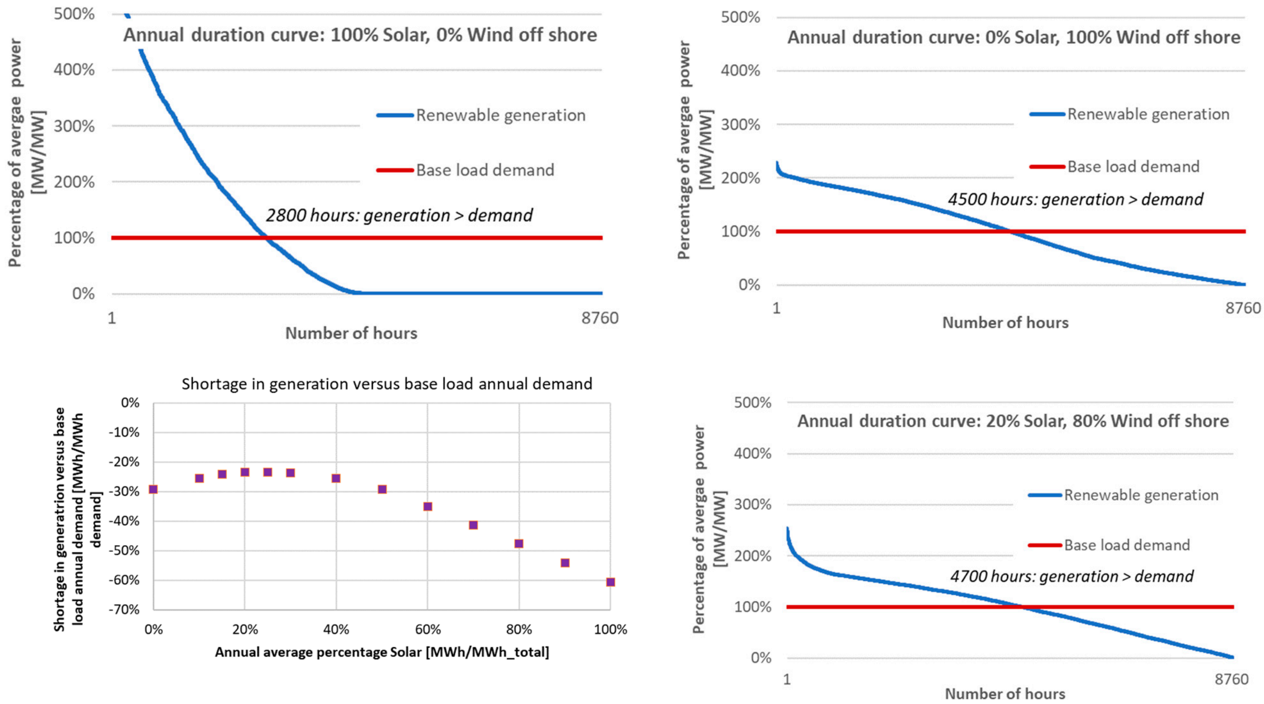

Figure 6. Analysis of renewable electricity generation (solar PV and wind offshore) annual duration curve versus a baseload demand.

The third figure, given on the bottom left, illustrates the effect of varying the percentage of solar in a renewable portfolio on the shortage of electricity, given in MWh annual generation by solar over the total demand. This figure shows that the smallest shortage in generation is achieved when the renewable energy portfolio consists of approximately 20% solar PV and 80% offshore wind. The shortage in this case is about 25%.

The bottom-right figure shows the annual duration curve of the optimal renewable energy portfolio of 80% offshore wind and 20% solar, which has a slightly better shape than the figure that only uses offshore wind. This optimal mix of wind and solar compares very well with comparable studies [41,42]. This figure also shows that for about 40% of the time, solar PV and offshore wind will not be able to meet demand.

2.6.2. Methodology of the Renewable Energy System Study

The zero-dimensional grid energy balance model has been programmed using the following rules:

1. Energy generation at any hour is calculated using the renewable generation portfolio from the ENTSO-E data times a correction factor, %VRE. The %VRE is 100%, as the total annual generation (MWh) equals the total annual demand (MWh); a %VRE of 110% indicates a 10% excess in generation (MWh) versus the annual demand
2. The balance between generation and demand is calculated for all hours.
3. In case of unbalance in generation and demand, first storage is utilized:
    a. In case of an excess in generation, the excess generation for that hour is stored in the energy storage.
    b. In case of a shortage in generation, the shortage is delivered by the energy storage.
    c. The filling and releasing of the storage take place within the technical parameters:
        i. Round-trip efficiency.

   ii. Storage volume (in MWh, based upon release of electricity).
   iii. Storage capacity (both for intake of electricity and release of electricity).
4. In case there is still a shortage in electricity at any hour, it is assumed that this electricity is generated by the backup power. In case there is still an excess in renewable production, it is assumed to be curtailed.

2.6.3. Optimal Levelized System Cost of Electricity for a Combined System of Renewable Generation and Storage

The levelized costs of electricity for a system consisting of a combination of renewable generation and energy storage has been calculated using the zero-dimensional grid energy balance model. The levelized cost of electricity is calculated for all cases in the following way (this is a slight simplification versus the detailed analysis in the first part of this paper):

$$LCOE\left[\frac{EUR}{MWh}\right] = \frac{C_{CAPEX} + \sum_n^N \frac{C_{OPEX}}{(1+r)^n} + \sum_n^N \frac{C_{EOL}}{(1+r)^n}}{\sum_n^N \frac{E_{consumed}}{(1+r)^n}} \quad (8)$$

In this system analysis, the costs for renewable power generation and storage are all investment (CAPEX) costs. The only variable costs (OPEX) are the operation and maintenance (O&M) costs of the renewable power generation and energy storage assets and the costs for backup power.

For the cost of the energy storage assets, the parameters from Table 1 are used. For the costs of renewable electricity generation, the cost parameters of Table 3 are used. As a simplification, the O&M costs are approximated as 2% of the CAPEX costs. The discount rate is taken as 8%, just as in the first part of this paper.

Table 3. Cost parameters of renewable energy generation [43].

	Offshore Wind	Solar PV
CAPEX (USD/kW)	2000	400
Annual O&M costs	2.5%	1.3%

2.6.4. Optimization Procedure

The minimum levelized costs of electricity from the total system ($LCOE_{system}$) have been determined for all cases. The parameters shown in Table 4 defining the energy storage and the amount of renewable energy (%VRE) are varied between the shown limits.

Table 4. Limits of the optimization parameters of the model regarding energy storage.

Optimization Parameter	Min.	Max.	
%VRE	100%	150%	Given as a percentage of annual average demand
Intake capacity of storage	0.1%	100%	
Release capacity of storage	0.1%	100%	
Volume of storage	1 h	200 h	Multiplied by the annual average hourly demand

3. Results

The results of this study are split up in part one, where the optimal storage for a given discharge duration and number of yearly cycles is found, and part two, where the results of part one are taken and integration into a fully renewable energy system is analyzed.

3.1. Part I: Comparison of Storage Technologies Using the Levelized Cost of Storage Methodology

In part one of this paper, the optimal energy storage is determined for both a fixed charging cost as well as charging at market price. In figures where different storage solutions are compared, the color intensity displays the $LCOE_{storage}$ difference with the second-best solution. The color intensity is calculated as follows:

$$I_{color} = 1 - \frac{LCOE_{storage,best}}{LCOE_{storage,secondbest}} \tag{9}$$

3.1.1. Fixed-Cost Analysis

The results of the fixed-price analysis can be seen in Figures 7 and 8. In these figures, the results of various scenarios are given depending on which energy storage technologies are available for the given location. The x-axis shows the ratio between stored energy and full discharge power (E/P ratio), which is equal to the discharge time at full power. The y-axis represents the number of yearly cycles during which the energy storage is used. Both axes are logarithmic. The possible combinations of yearly discharge cycles and the E/P ratio are limited to the total number of hours in a year, shown by the triangular shape of the figure. At the border between the white upper triangle and the indicated energy storage technologies, the energy storage is continuously in operation, either charging or discharging. The more inwards towards the origin, the less the storage is utilized.

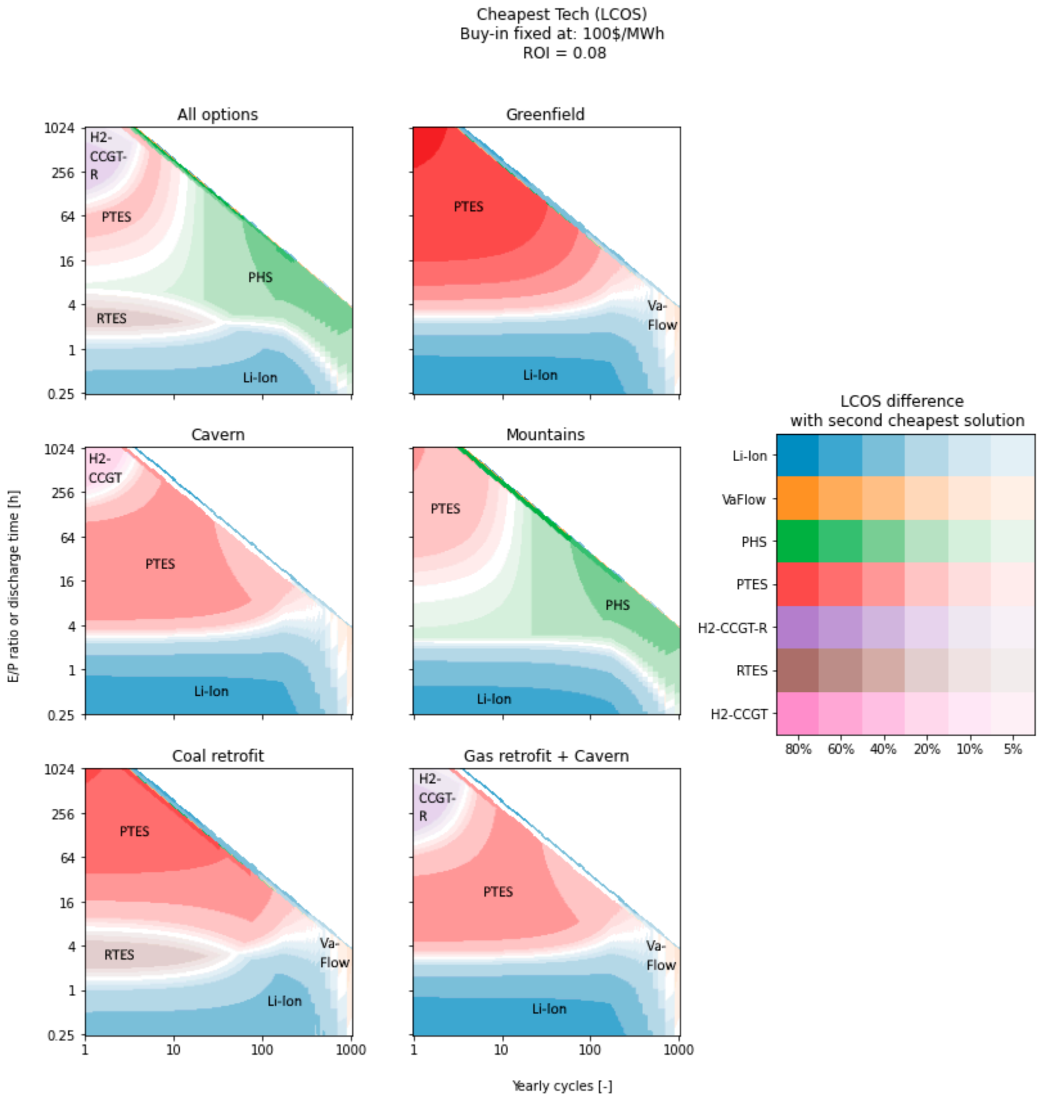

Figure 7. The economically most attractive storage technology for various location scenarios (see Table 2) and a fixed electricity buy-in price of USD 100/MWh. The intensity of color variation is explained in Equation (9).

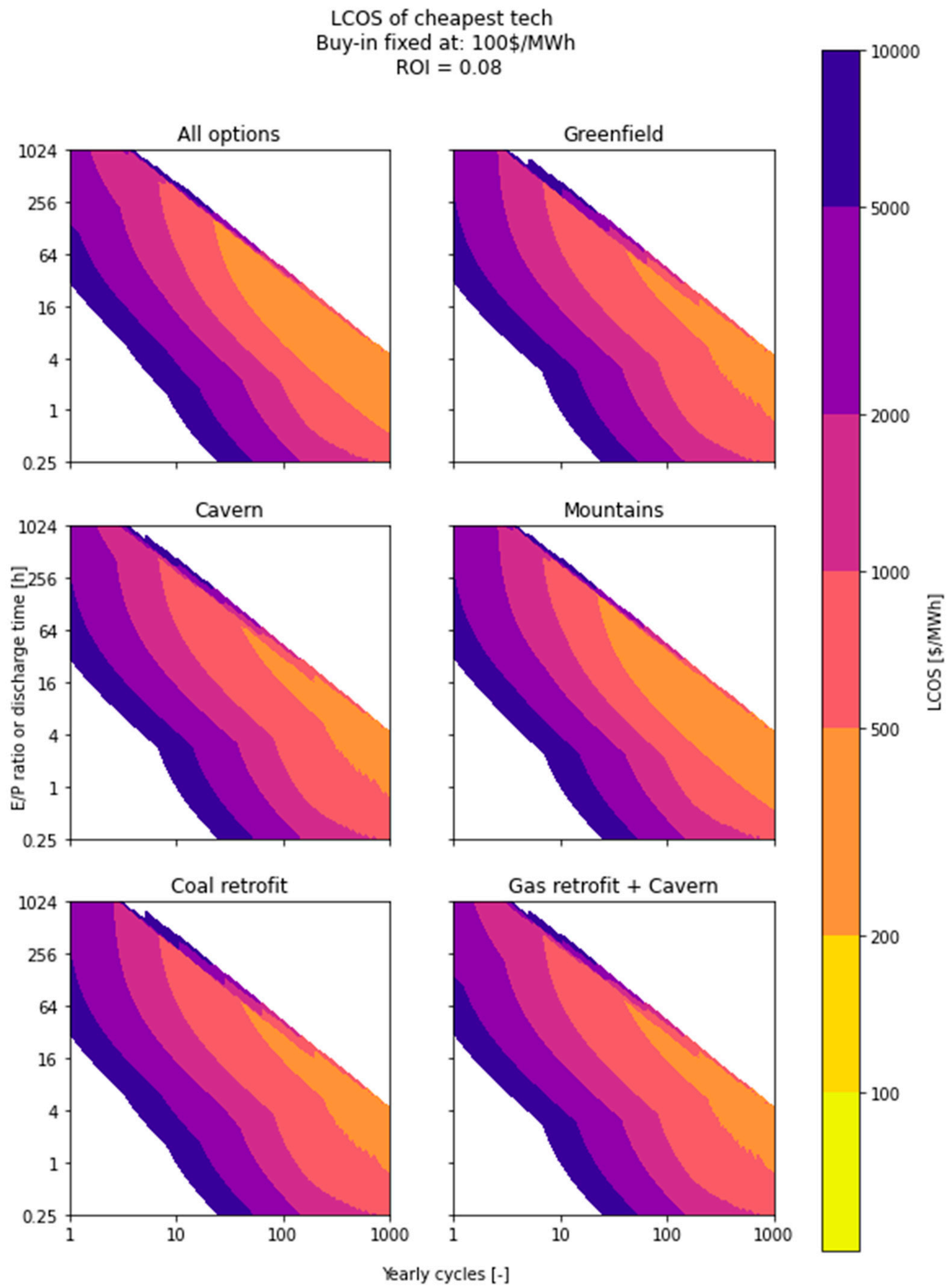

Figure 8. The $LCOE_{storage}$ of the optimal solution; note the logarithmic scale. $LCOE_{storage}$ values above USD 10,000/MWh are not displayed.

The power price is fixed in this first analysis to USD 100/MWh.

Seven technologies are most prominent. Li-ion batteries are most prevalent for short-duration storage under 4 h and when no geographical features are present. Pumped Hydro Storage (PHS) remains the best option for medium-duration storage if the right geographic conditions are present. Pumped Thermal Energy Storage (PTES) appears to be the economically most attractive solution for medium-to-long-duration energy storage if Pumped Hydro and hydrogen storage are not possible. All hydrogen-based technologies are best used for seasonal storage, and a retrofit is preferred if available. RTES provides a potentially attractive option for medium-duration storage for a lower capacity factor.

The resulting $LCOE_{storage}$ can be seen in Figure 8. This figure shows that an $LCOE_{storage}$ of USD 200–500/MWh can be achieved for storage with a high number of annual cycles. Seasonal energy storage, with a low number of cycles and longer duration of discharge, will be more expensive, typically USD 500–1000/MWh as a minimum.

3.1.2. Dynamic Price Analysis

The retrospective lowest possible charging price algorithm has been applied for all technologies on the EPEX SPOT prices of 2023, accessed via the ENTSO-E Transparency Platform. The average price for 2023 was USD 162.95/MWh. The power buy-in price of the RLPCP algorithm is lower than the average price, as buy-in happens at a strategic point in time, when prices are low. The RLPCP price varies for every storage technology and implementation, as the RLPCP price is a function of RTE, E/P ratio, and the number of yearly cycles.

The results, expressed as the most economically attractive storage technology, of the RLPCP algorithm for market prices are compared with the results for the fixed charging price (USD 100/MWh) in Figure 9. The plot on the left displays all technologies, while the plot on the right only shows geographically independent storage options. The color intensity displays the $LCOE_{storage}$ difference with the second-best solution.

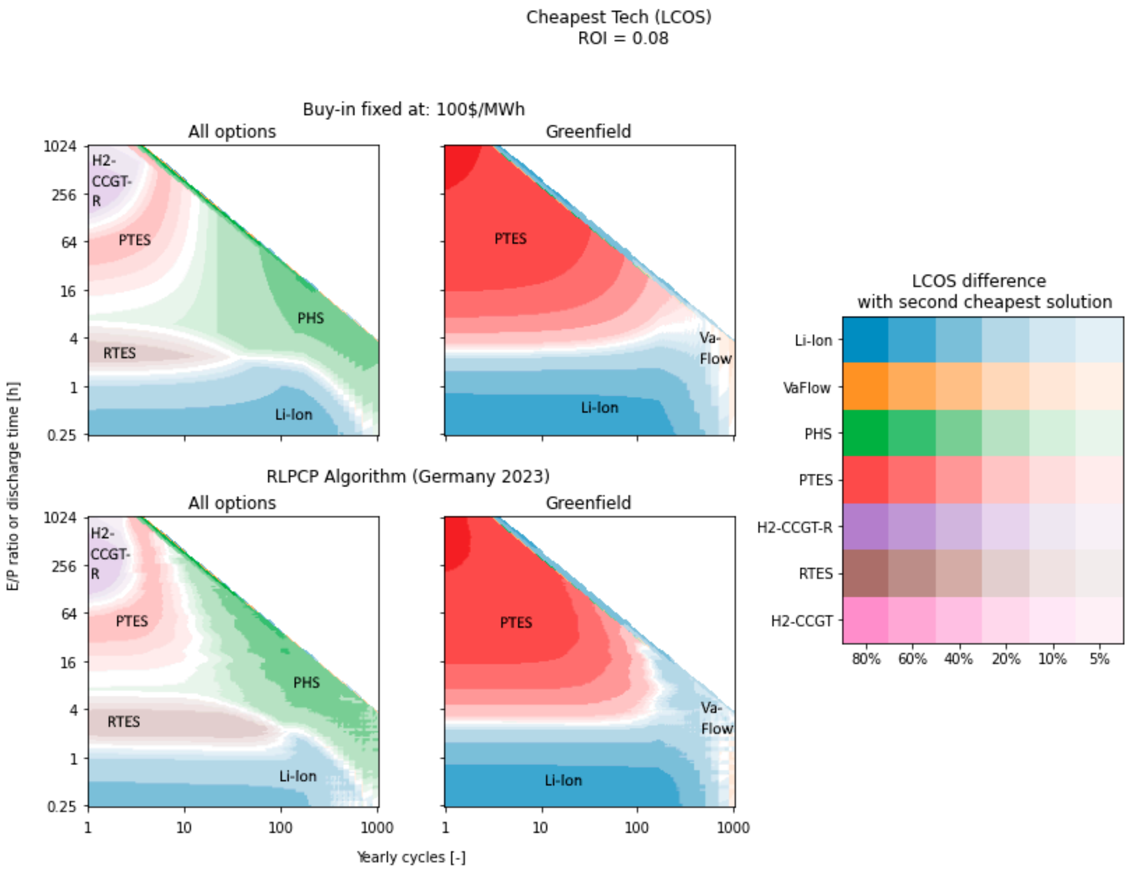

Figure 9. Results of the model using the RLPCP algorithm shown above compared to the results of the fixed buy-in price of USD 100/MWh below; color intensity indicates distance from second-best solution.

Figure 9 shows that by using the RLPCP algorithm, the areas of the respective best technologies are less regular, yet the main trends remain. One difference is that when real power prices are considered, a lower capacity factor, meaning less use of the energy storage, which can be found towards the origin, slightly favors less efficient storage technologies, while a higher capacity factor favors more efficient technologies.

Figure 10 shows the levelized cost of storage for the chosen solution, shown in Figure 9. The $LCOE_{storage}$ here also includes buy-in of electricity as calculated using the RLPCP algorithm. All values of $LCOE_{storage}$ higher than USD 10,000/MWh are deliberately left out. Again, the upper two figures show the results of the RLPCP algorithm, and the lower two figures are calculated with a fixed USD 100/MWh buy-in price.

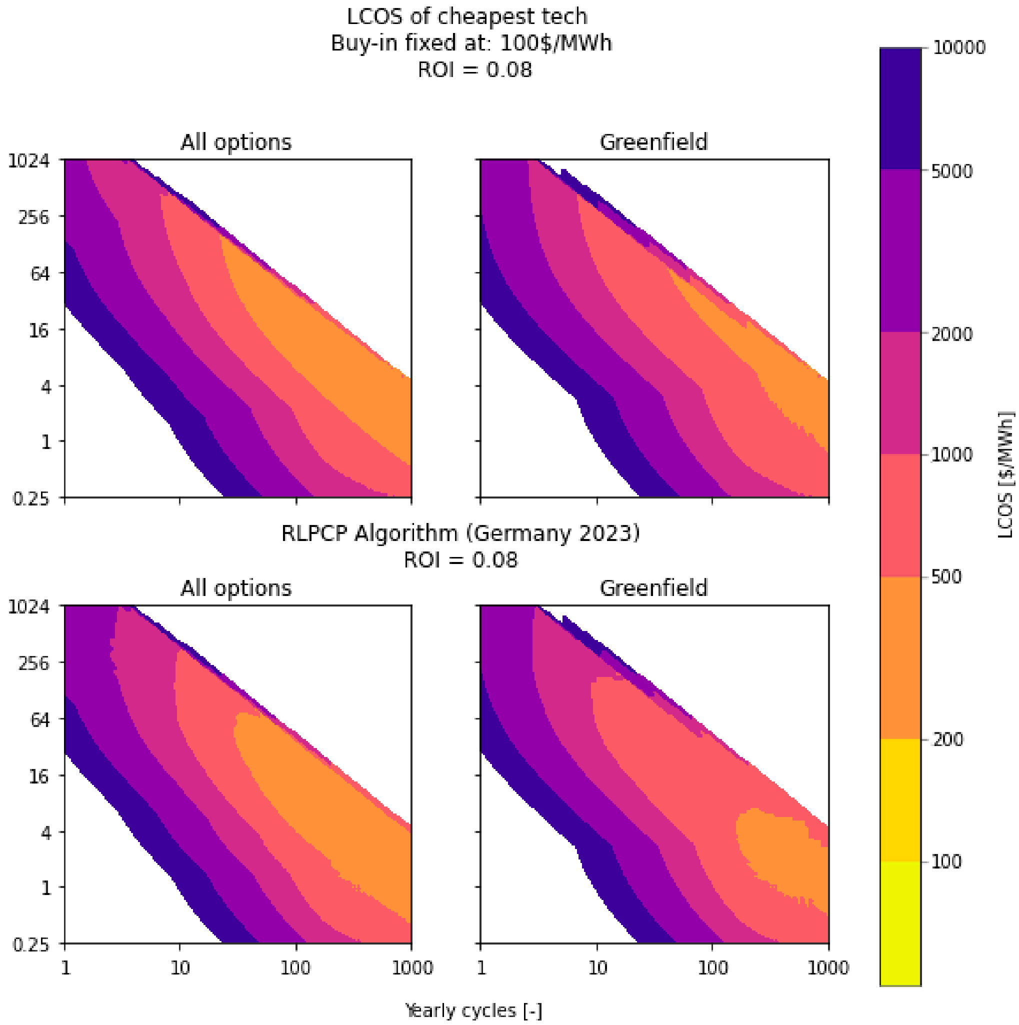

Figure 10. $LCOE_{storage}$ of found optimal solutions, using the RLPCP algorithm shown above, compared to the results of the fixed buy-in price of USD 100/MWh below.

It can be observed that a higher utilization of the storage allows for a lower-level LCOE. Furthermore, it shows that the greenfield scenario has a definite disadvantage over the full range of choice. According to this model, an $LCOE_{storage}$ between USD 200/MWh and USD 500/MWh could be reasonable if the capacity factor is sufficiently high. Prices are slightly lower compared to a fixed USD 100/MWh buy-in price as low or negative prices are leveraged; however, the outcome is largely similar.

3.2. Part II: Energy Storage in a Fully Renewable Electricity System

In the first part of this paper, an optimal solution is found for a known number of yearly cycles and discharge times. In the second part of this paper, integration of energy storage in the energy market in northwestern Europe is analyzed such that an expected power price and amount of storage for a fully renewable energy system is found.

3.2.1. Time/Frequency Analysis of the Energy Balance in a 0D Grid Model

A 0D grid model has been used to calculate the number of required cycles per year for energy storage. In this case, the energy storage is modelled with a 100% round-trip efficiency, intake, and release capacity equal to the annual average demand load and an infinite storage volume. The total renewable power generation annual volume is modelled to be equal to the total annual offtake volume; therefore, %VRE = 100%. The demand is modelled as a baseload. All storage release events are grouped in bins for the duration of the release. In this way, bins are created with the number of release cycles per year and the average duration of the release cycle. The following bins have been created: hourly (1–4 h), intraday (4–16 h), multiday (16–64 h), weekly (64–128 h), and multiweek (128–256 h). Figure 11 shows the number of yearly cycles (right axis) and the total amount of annually discharged energy for these bins (left axis) for the year 2023.

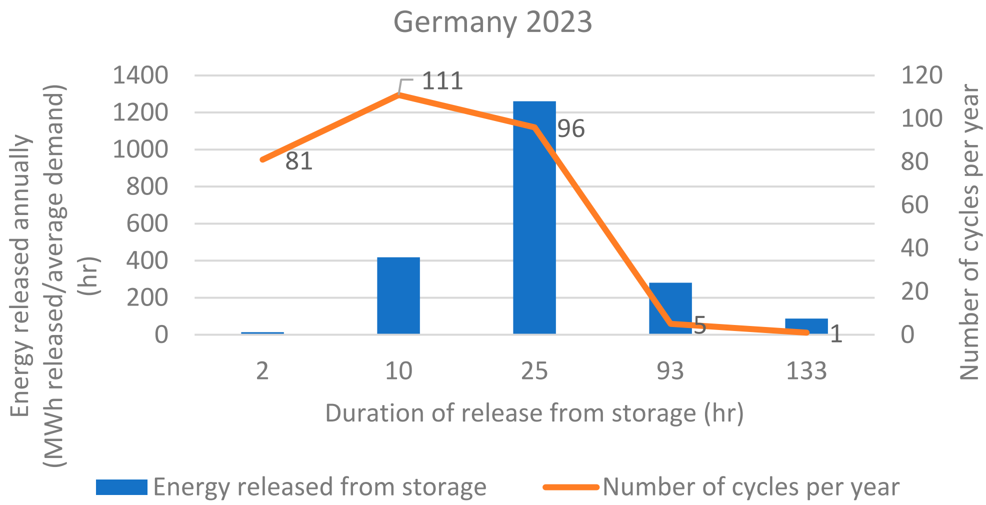

Figure 11. Distribution of the release cycles from the storage grouped per bin of duration. On the left axis is plotted the total energy released annually from the storage (per duration bin) and on the right axis is the number of annual events. The average duration of the release of the bin is shown on the *x*-axis.

The bins are indicated on the *x*-axis with the average duration of release. For example, 25 h is the average release time in the 16–64 h bin, and 93 h is the average release time in the 64–128 h bin. This figure shows that the annual number of events decreases with the average duration of release, except for the short-duration releases. The largest volume from storage is released with an average duration of 25 h. About half of the volume of the energy released from the storage is released on this time scale. The energy storage cycles with a shorter time duration show a much lower volume. There is only one cycle with an average duration of 133 h, or just over 6 days; these are linked to longer periods of shortages of wind and solar generation. This analysis shows that an optimal storage volume is likely to be between 25 and 93 h, as this can also cover the smaller time scales. Figure 12 shows the same analysis for the years 2021 and 2022. There are only slight differences between these years and the data for 2023. Based on this comparison, the data for 2023 are used as input for the analysis.

This frequency analysis of the storage capacity is combined with the plots for the economic optimal $LCOE_{storage}$ from part one of this paper. Figure 13 shows how these bins are located within the $LCOE_{storage}$ plots from the first part of this paper. The most promising technologies that appear from this analysis are the Li-ion or RTES for the short duration (1–4 h), PHS, PTES, and RTES for medium duration (4–128 h), and retrofit (H2-CCGT-R) for long duration (128+ h).

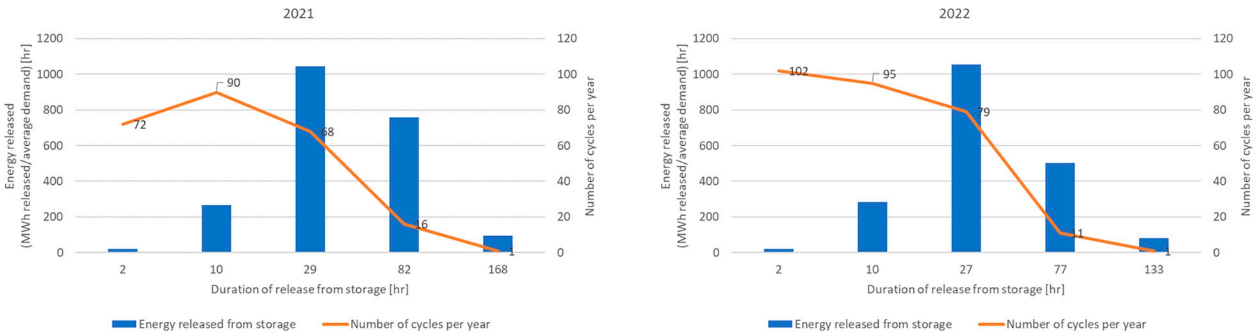

Figure 12. Total annual energy and number of cycles of the release cycles from the storage grouped per bin of duration, evaluated for the years 2021 and 2022.

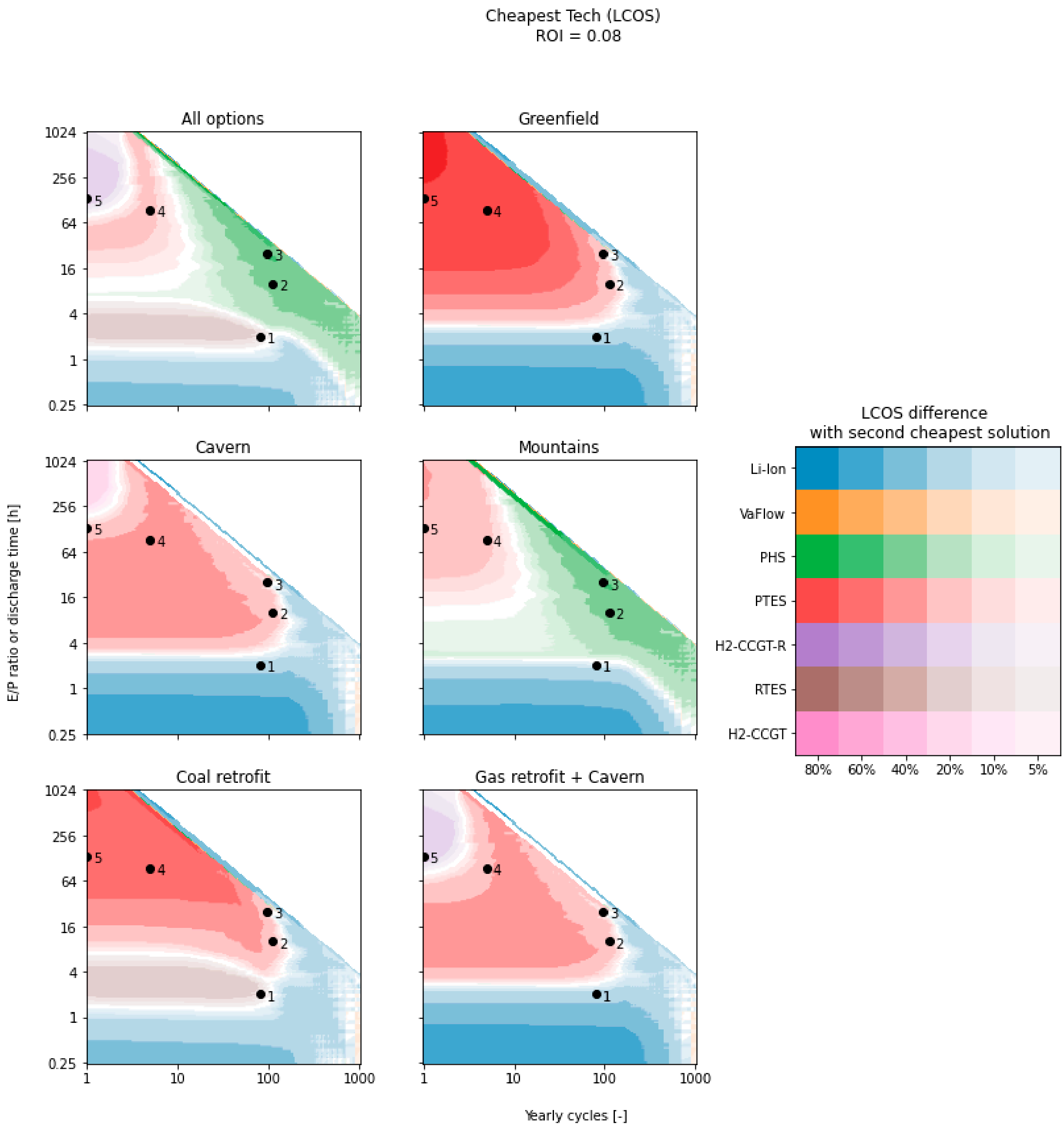

Figure 13. The economical best technology, based on the RLPCP algorithm, combined with the frequency analysis for storage. 1: 1–4 h, 2: 4–16 h, 3: 16–64 h, 4: 64–128 h, 5: 128–256 h.

A further analysis has been performed for the calculation of the $LCOE_{storage}$ of the different technologies for the different frequencies that have been identified. Table 5 shows the $LCOE_{storage}$ for these cases, shown in Figure 13. $LCOE_{storage}$ values above USD 4000/MWh that are not in the top five choices are removed from this table for readability.

Table 5. $LCOE_{storage}$ for discharged stored energy, including the charging cost of the current market for the points determined in the frequency analysis. The colors indicate the top five most attractive forms of energy storage (within the top five, green is most attractive and red is less attractive) per energy storage release time bin. The options outside of the top 5 are indicated by a light grey font color.

E/P Ratio (h)	2	10	24	93	133
Yearly Cycles (-)	**81**	**111**	**90**	**5**	**1**
Li-Ion	944	657	825		
NaS	2429	1382	1640		
LeadAcid		2575	2960		
VaFlow	1816	1015	1228		
PTES	1152	562	731	1449	5433
dLAES	3922	1442	1509		
RTES	848	962	1378	3689	
PHS	1018	330	385	1708	7489
aCAES	2001	699	838	2630	
dCAES-H2	2591	1088	1400	3037	
H2-CCGT		1818	2177	2481	6377
H2-FuelCell		2662	3120	3634	9426
H2-CCGT-R	2552	1585	2069	1928	4442

Table 6 shows the $LCOE_{storage}$ of the storage technologies without the charging cost. This reflects a future energy system in which charging of storage is always preferred due to an abundance of renewable energy.

Table 6. $LCOE_{storage}$ for discharged stored energy excluding charging cost for the points determined in the frequency analysis. The colors indicate the five most attractive forms of energy storage (within the top five, green is most attractive and red is less attractive) per energy storage release time bin. The options outside of the top 5 are indicated by a light grey font color.

E/P Ratio (h)	2	10	24	93	133
Yearly Cycles (-)	**81**	**111**	**90**	**5**	**1**
Li-Ion	950	518	563		
NaS	2437	1168	1237		
LeadAcid		2387	2599		
VaFlow	1822	817	855		
PTES	1142	201	121	1191	5369
dLAES	3930	1317	1251		
RTES	797	229	202	3174	
PHS	1023	195	130	1592	7459
aCAES	1992	356	220	2364	
dCAES-H2	2570	443	262	2584	
H2-CCGT		609	293	1650	6104
H2-FuelCell		942	494	2461	8977
H2-CCGT-R	2470	376	185	1096	4170

From Table 5, Table 6, and Figure 13, it can be concluded that for long-duration storage (multiple days to weeks), the H2-CCGT-R is the most economical solution if the cost of buy-in energy is free, but this option is still relatively expensive (+−USD 2000/MWh). In this case, this solution also performs quite well for the medium duration (one to several days). When the energy buy-in price of the current market is included, the low efficiency is a large financial penalty for this technology, but it is still one of the only options for this long-term storage.

The Pumped Thermal storage is the best economic solution for several hours to several days of storage, but it is in close competition with Pumped Hydro, aCAES, and H2-CCGT—retrofit.

Alternative battery technologies, such as NaS and VaFlow, are much more expensive than thermal, mechanical, and hydrogen storage options. They might be attractive for storage for several hours and up to one day, but they are in close competition with Li-ion batteries.

It should be noted that these conclusions are only based on economic value. Several other considerations arise when deciding on an energy storage technology, such as local possibilities, sustainability, footprint, safety, and societal opinion.

3.2.2. Comparison of $LCOE_{system}$ and $LCOE_{storage}$ for Single Storage Technologies

In this analysis, different systems with a single storage technology are compared. Per storage technology, the system is optimized for the minimum $LCOE_{system}$ of the system. A relatively high cost for backup power of USD 1000/MWh is assumed to minimize the utilization of backup power. This cost level of backup power is based on the analysis shown in part one of this paper. Figure 14 shows the impact of storage on the system LCOE with only a single storage technology. Figure 15 shows the storage volume and backup power demand with only a single storage technology. $LCOE_{system}$ is the levelized costs of electricity consumed in the total system, $LCOE_{storage}$ is the levelized cost of the electricity delivered by the storage, and $LCOE_{generation}$ is the levelized cost of the electricity delivered by the renewable generation without curtailment.

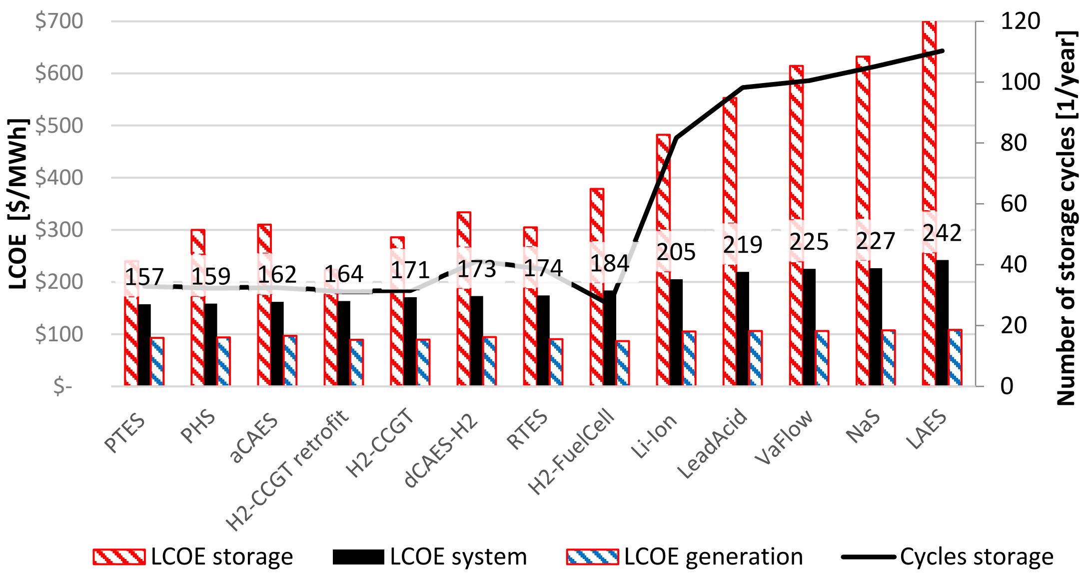

Figure 14. System LCOE comparison in a fully renewable system for a single storage technology. The technologies are ranked based upon levelized costs of electricity consumed in the system ($LCOE_{system}$). The displayed numbers are also the LCOE in USD/MWh. The number of cycles is calculated by dividing the annually released volume from the storage by the storage volume.

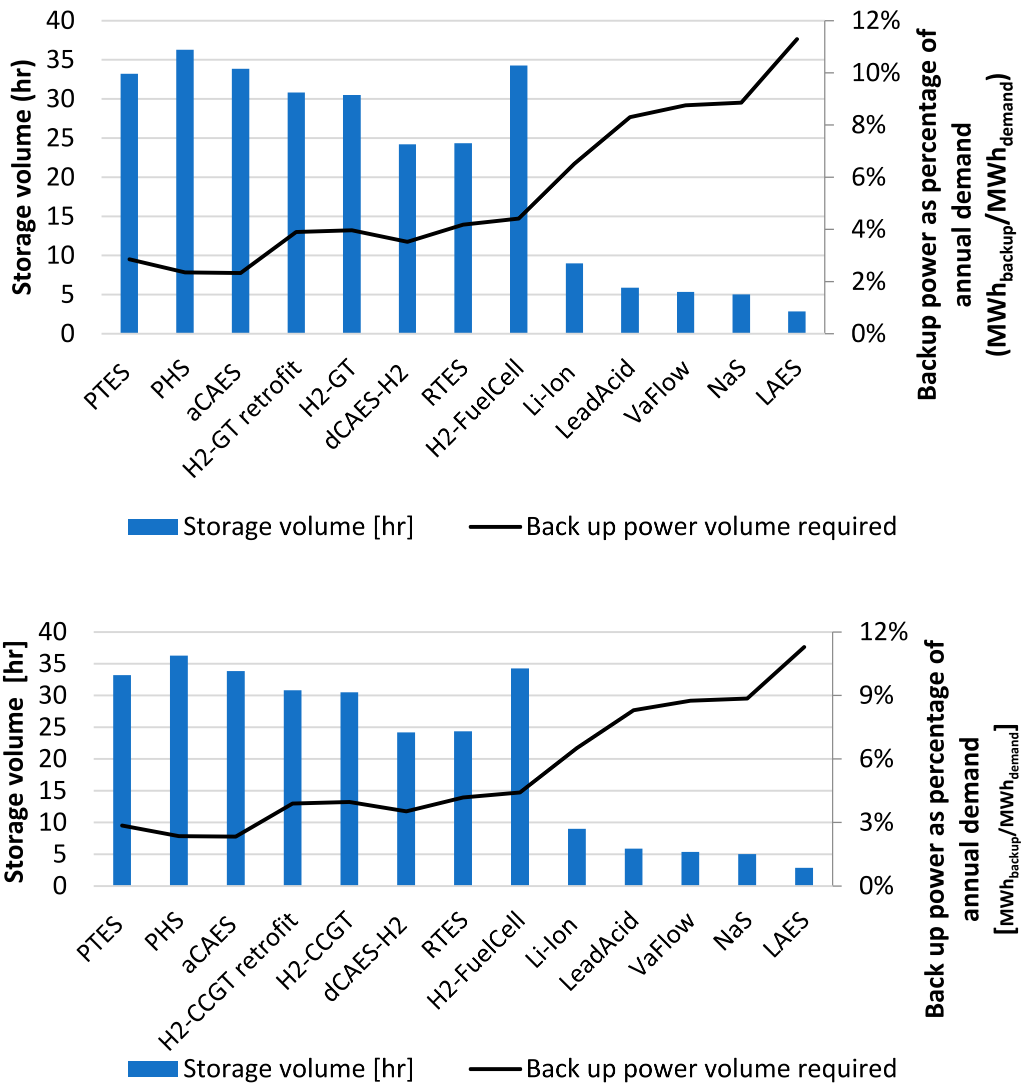

Figure 15. Storage volume and backup power demand in a fully renewable system for a single storage technology. The same sequence of technologies as in Figure 14 is used.

The $LCOE_{system}$ varies between USD 157/MWh and USD 242/MWh. In the latter case, a significant part, up to 12%, of the shortage in generation is generated by expensive backup power. In the cases with the lowest $LCOE_{system}$, the backup power is only required for 2.4% of the volume. The $LCOE_{storage}$ starts at USD 240/MWh for PTES and increases above USD 800/MWh for the battery options and LAES.

It is interesting to see the distinction between the technology types, as the lowest costs are for PTES, PHS, and A-CAES, and all of these storage methodologies are based upon mechanical and/or thermal cycles. The hydrogen-based technologies can also be seen as one group, with the hydrogen retrofit CCGT as the best option in close competition with the diabatic CAES with hydrogen as a fuel. The converted thermal power plants (RTES) perform slightly worse than the hydrogen options.

All batteries have a significantly higher LCOE than the other options. They are not optimal for long-duration energy storage but perform much better on a shorter scale of up to a few hours. LAES is the most expensive option, although this option is intended for longer periods of energy storage.

The most economic energy storage technologies all have a storage volume of about 40 h. The total discharge from the storage is about 30 times the storage volume. The optimal charging and discharging capacities of the storage (not shown here) are just below the average annual demand.

The backup power is mainly used to overcome longer periods of shortage of renewable generation. Figure 16 shows as an example the content of the storage volume and the amount of backup power applied in the case of PTES. This figure shows that there are six big events on an annual basis when backup energy is needed to prevent blackouts.

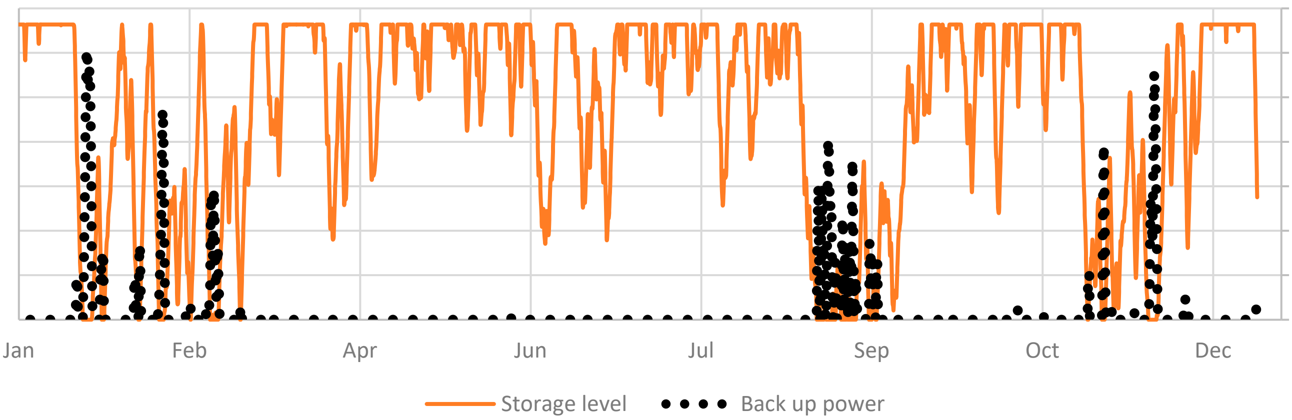

Figure 16. Storage level and amount of backup power used over the year of the analysis for the case of the single storage technology PTES used.

3.2.3. Balance between Excess Renewable Generation Capacity and Storage Capacity

An important parameter in the analysis is the capacity of renewable power. The $LCOE_{generation}$ of renewable energy (USD 80–100/MWh) is significantly lower than the $LCOE_{storage}$ (USD 250–500+/MWh). An increase in renewable power (%VRE in the model) results in a reduction in the requirement for storage and backup power.

In the following analysis, the impact of %VRE on the $LCOE_{system}$ and the percentage of backup power is studied for the PTES storage case. This analysis, shown in Figure 17, shows that above about 130% %VRE, the impact of %VRE on the $LCOE_{system}$ is limited, and the increase in %VRE decreases the requirement for backup power.

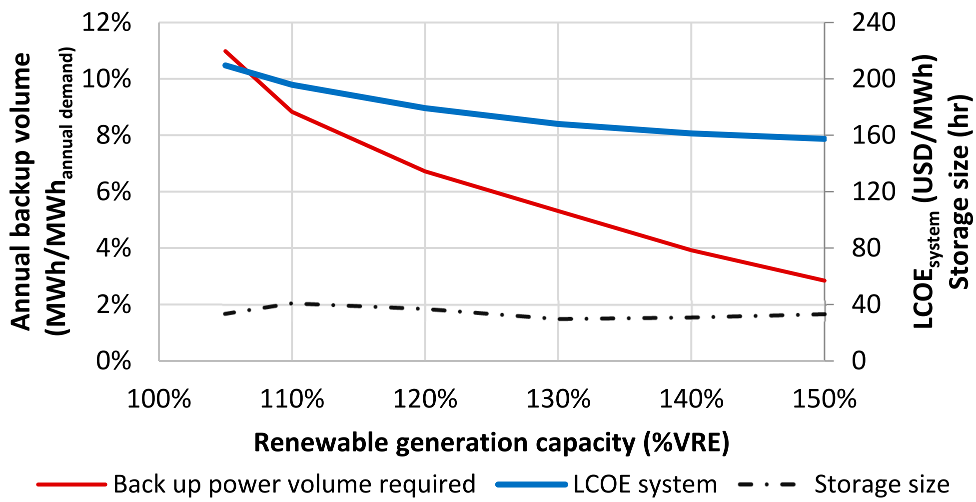

Figure 17. Sensitivity of storage capacity, system cost, and backup power demand to renewable generation capacity.

The optimal storage volume is not overly sensitive to the amount of renewable generation capacity, as it remains around 30 h of storage. The storage, however, is used more efficiently with a higher excess of renewable electricity available.

3.2.4. Sensitivity to Flexibility in Demand

Lastly, the effect of flexibility in demand is investigated. Currently, flexibility in energy demand is already being studied and applied in the form of heat storage for district heating, smart charging of electronic vehicles, flexible power offtake agreements for industrial users, and more. Numerous studies have already pointed out how implementing flexibility may increase the market value of renewables and may provide a means to accelerate the energy transition without additional large capital investment [39,44]. One of the potential drivers of flexibility could be the increase in electric vehicle EV capacity combined with flexible charging models, such as V1G or V2G [45].

Flexibility is modelled as a percentage of the actual demand at any hour. A flexibility of 10% therefore assumes that the load can vary by 10% up or down. The priority of extra demand in the 0D grid model is placed before intake by the storage. The demand load will therefore be reduced if there is a disparity between generation and demand at any moment. This will be prioritized before releasing electricity from the storage. Extra load demand will be prioritized before storing energy in the storage.

This analysis, shown in Figure 18, shows that an increase in flexibility in demand reduces the LCOE costs from USD 150/MWh to USD 100/MWh at 50% flexibility. The decrease in system costs is nearly linear with the flexibility in demand. The main reason for this reduction in system costs is the increase in direct utilization of renewable electricity. Therefore, there is a reduction in demand for renewable generation capacity (%VRE), which is reduced from 150% to 117%. Furthermore, storage volume is reduced from 30 h to 10 h. The requirement for backup power is also significantly reduced from 2.9% to 1.4% by the increase in flexibility in demand.

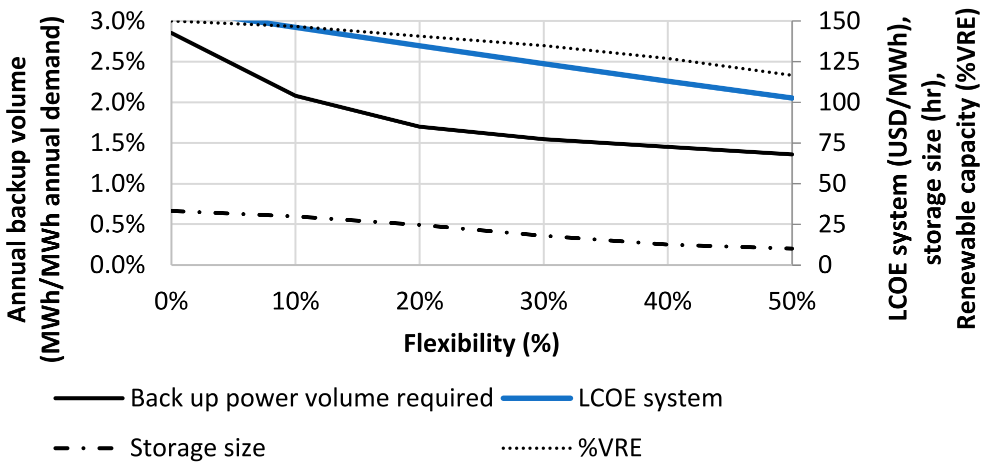

Figure 18. The effect of flexibility on LCOE of the modelled 0D energy grid with PTES as the storage option.

4. Discussion

4.1. Impact of the Electricity Buy-In Price

To check the sensitivity of the model to the electricity buy-in price, a constant USD 50/MWh buy-in price is used in a second analysis. It is seen in Figure 19 that there are no substantial changes in the ranking of the optimal solutions. There is, however, a slight bias towards energy storage solutions with a lower round-trip efficiency (e.g., RTES) compared to the fixed-price scenario.

The minimum $LCOE_{storage}$ does drop only slightly, as can be seen in Figure 19. A very significant part of the energy storage costs is the CAPEX costs. The charging cost has a relatively limited effect and scales with RTE.

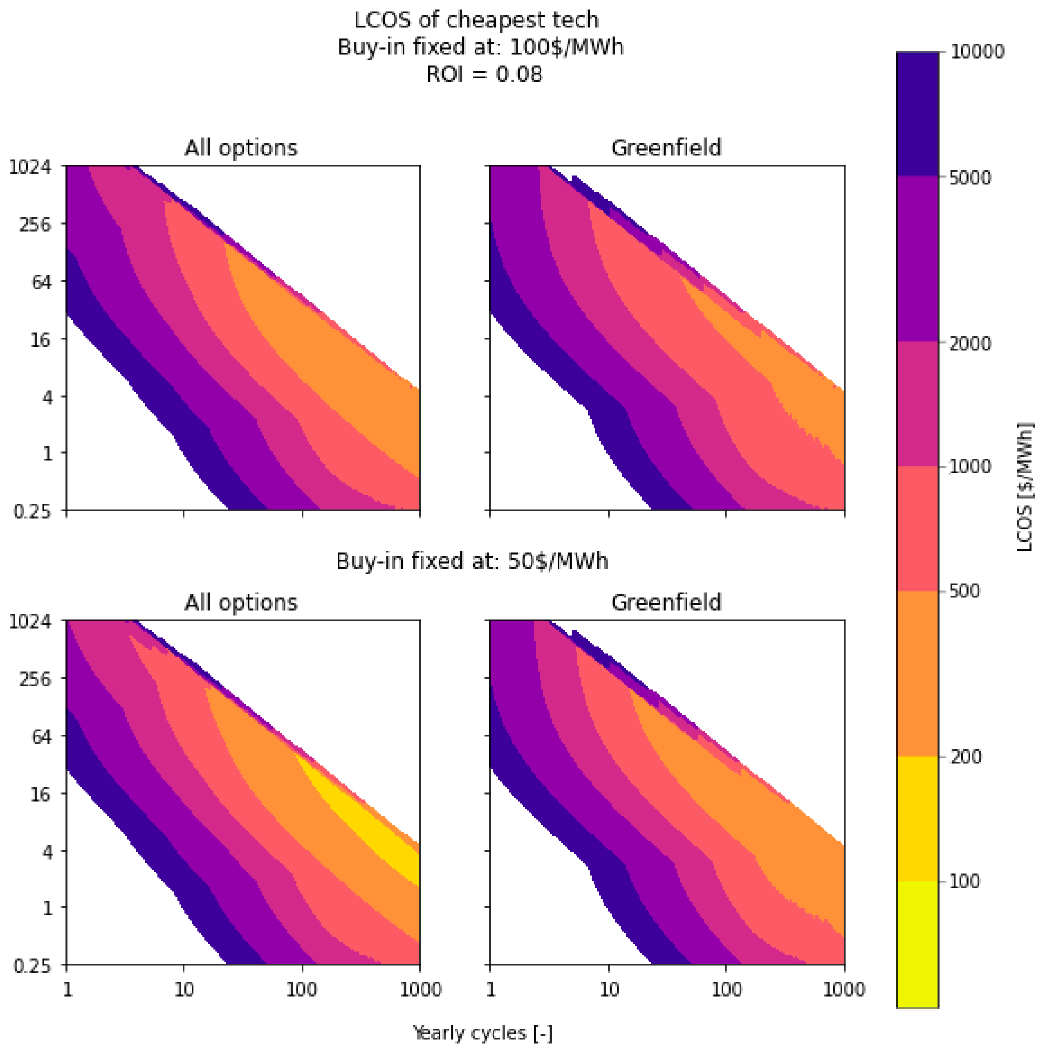

Figure 19. Minimum $LCOE_{storage}$ for USD 100/MWh buy-in price compared to USD 50/MWh.

4.2. Influence of a Significant Reduction in CAPEX Costs on the Levelized Cost of Storage

While all cost data given in this paper are a best estimate of the future cost, some cost datapoints are especially disputed. In this section, the sensitivity to changes in CAPEX is evaluated to enable more robust conclusions. Figure 20 shows the energy storage landscape for greenfield and unrestricted location scenarios, where the price of lithium-ion batteries has dropped by 25% and 50%. According to current projections, a 25% price drop compared to current values is to be expected before 2030. A 50% price drop is estimated to happen around 2045 [46].

Li-ion batteries are now more prevalent in the energy storage landscape. Still, for above 4 h of storage time, PHS, PTES, and hydrogen solutions remain undefeated.

Alternatively, it may be argued that as PTES is still in an early stage of development, CAPEX may be higher than expected. Figure 21 displays the solutions for PTES with 150% CAPEX as well as 200% CAPEX.

While the solution does change, the general conclusions remain the same. It can therefore be concluded that the model is relatively robust to changes in CAPEX if the results are regarded as an indication of trends rather than an actual prediction of prices.

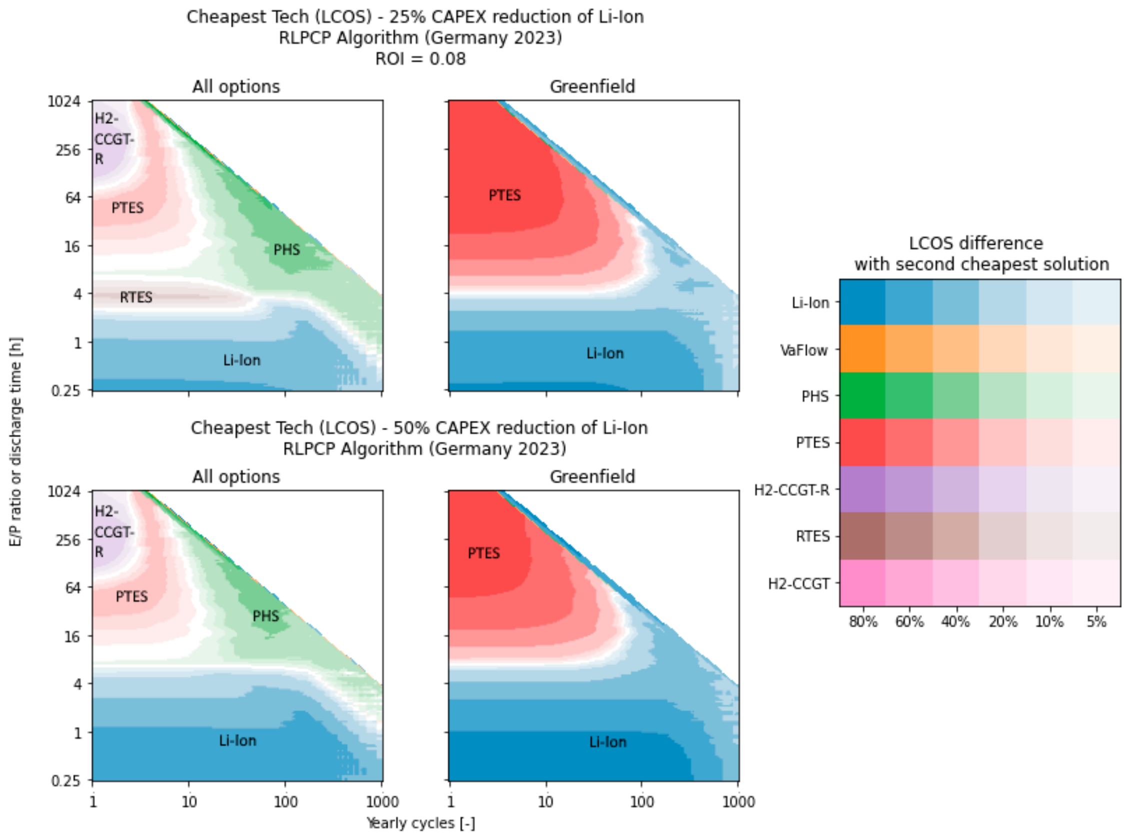

Figure 20. Best technologies based on $LCOE_{storage}$ for a 25% and 50% decrease of Li-ion CAPEX.

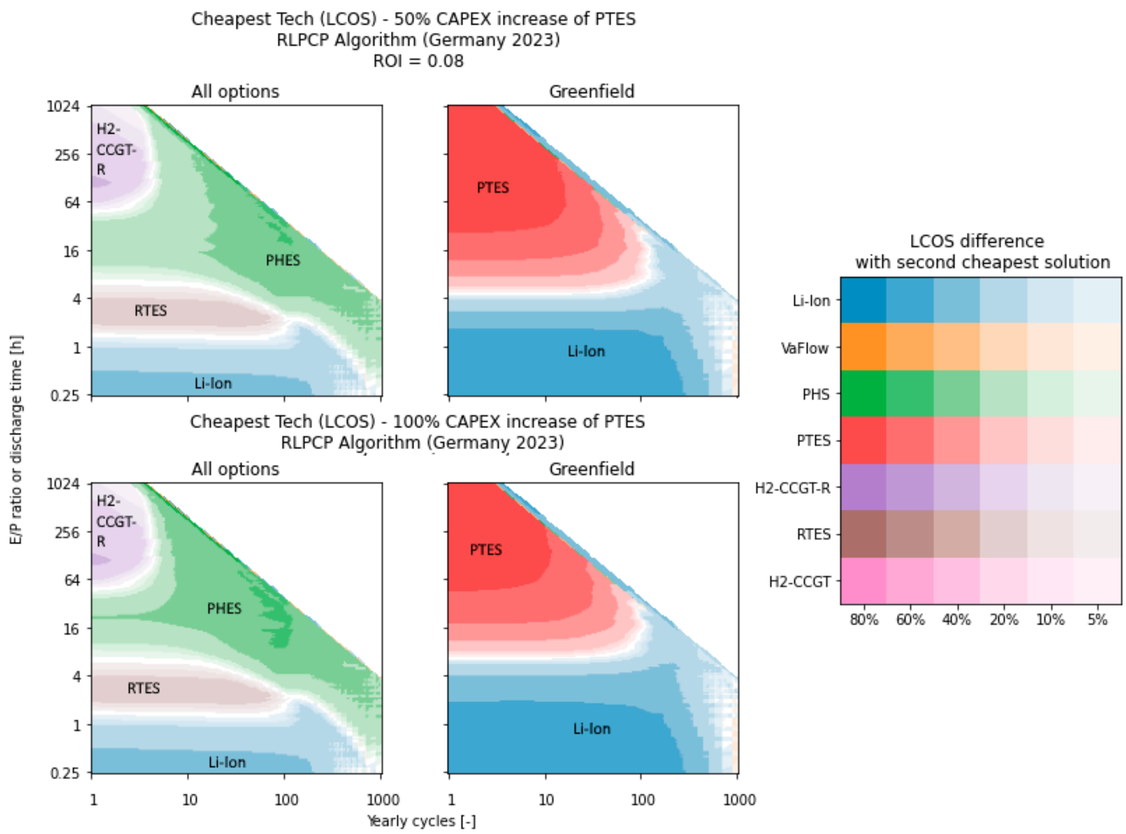

Figure 21. Best technologies based on $LCOE_{storage}$ for a 50% and 100% increase of PTES CAPEX.

4.3. Second-Best Technologies for the Levelized Costs of Storage

As most technologies are not very distant from the second economically most attractive technology, it is also interesting to look at these solutions, as shown in Figure 22. After all, there may be many considerations beyond economical ones that go into choosing the best energy storage solution. The RLCCP algorithm has been used to calculate the charging price.

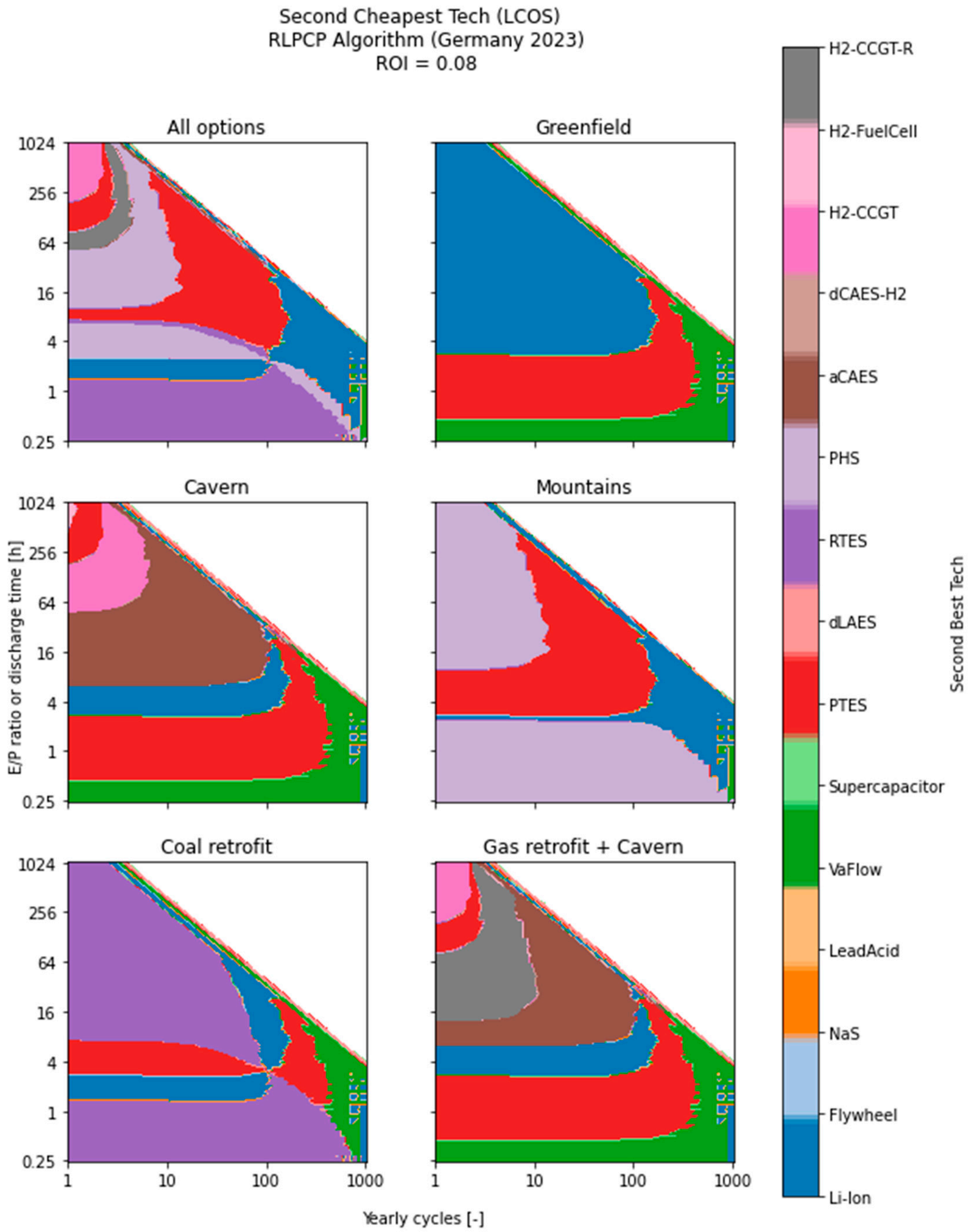

Figure 22. Second-best solution for energy storage using the RLPCP algorithm.

In Figure 22, a much wider range of options is displayed. These technologies are also valuable to consider as they might show more desirable characteristics depending on the project.

4.4. Further Considerations

The presented research comprises a high-level levelized cost of electricity study to rank different energy storage options for different time scales. Local and project-specific details and economics will influence the calculated LCOE and might influence the ranking. Non-economic aspects have not been taken into consideration in this study. The CAPEX numbers are estimates for the 2030 situation based upon a broad literature study, and the real CAPEX might of course differ significantly from these numbers. The presented results in the second part of this paper for the fully renewable system are applicable to offshore-wind-dominant generation, as in northwestern Europe, but the methodology can be applied to other renewable energy systems.

In the methodology in the first part of this paper, only full cycles at full load are considered. Realistically, it could be beneficial to run smaller cycles or at part load. This could affect prices. Therefore, for long-duration storage, the RLPCP algorithm is not quite realistic. As power prices are only a small part of the total storage cost, this is assumed to be an acceptable solution, as it still captures the dynamics of charging at low power prices, which is beneficial for technologies with a lower round-trip efficiency and a low number of yearly cycles.

The numbers given in Table 1 may vary by project and geographical location. As some of these technologies are not yet very mature, the cost can be regarded as the best estimate for when these technologies will be implemented. The results should therefore be interpreted as a qualitative indication of trends, rather than quantitative predictions.

The optimal renewable portfolio includes offshore wind, but this is not attainable for all countries. On-shore wind is not considered, as offshore wind has a more beneficial capacity factor. Use of on-shore wind or a different renewable portfolio may impact prices.

In contrast to many other studies, no detailed information about geography, the electrical grid, or existing assets is incorporated in this research. Therefore, no specific conclusions for a specific geographic area or system transition steps can be derived from it.

The outcomes of this research are well in line with other publications, like *Monetizing Energy Storage* by Schmidt and Staffel, in which a nice overview is presented of the state of the art of energy storage. The calculated optimum size of storage of the current research is slightly higher than in the work presented by *Monetizing Energy Storage*, as fossil backup power is assumed to be relatively expensive in this research and thereby minimized. The effect of flexibility, the share of renewables, and the LCOE compare very well with the results presented [47].

The analysis presented in this paper can serve as a decision-making tool for industry stakeholders and policymakers and highlights the paramount role of energy storage in a sustainable energy future.

5. Conclusions

Three methods were used to rank electricity storage technologies: fixed charging price, market-based charging price, and integration into a fully renewable energy system. The comparison of the three methodologies shows a robust economic ranking of the technologies.

For electricity storage for one to several days, there is close competition between Pumped Hydro Storage (PHS), Pumped Thermal (PTES), and hydrogen application in a retrofitted gas-fired power plant (H2-CCGT-R). The retrofitted gas-fired power plant using hydrogen (H2-CCGT-R) is overall the best performer for storage duration of several days. Li-ion batteries appear to have relatively limited economic value for longer-term storage. They have their value mostly in short-term balancing of the grid (below typically 1–4 h time scales).

In a fully renewable electricity system, most storage is typically required at a time scale of one to two days (30–40 h). The PTES, PHS, and H2-CCGT retrofit options are all good candidates for this. An interesting technology that was not included in many other research papers is Pumped Thermal Energy Storage (PTES). This technology performs relatively well in the one- to multi-day storage time scales.

The levelized costs of the electricity released from storage ($LCOE_{storage}$) are found to be in the order of USD 200–1000/MWh. This is significantly higher than the typical $LCOE_{generation}$ from renewable sources (USD 50–100/MWh). Fewer cycles per year allow for charging the storage at lower prices; however, the charging cost is only a fraction of the total cost, and the lower capacity factor will increase the price much more than the effect of a lower charging cost. The effective overall levelized costs of electricity of a fully renewable system start at USD 150/MWh when the most economic storage technologies are implemented.

Both Pumped Thermal Energy Storage (PTES) and Pumped Hydro Storage (PHS) appear as the most economically attractive options in this study. However, both options have their challenges: PHS is geographically constrained, and options for new PHS in industrialized societies are limited. Pumped Thermal Energy Storage is a technology under development without large-scale demonstration available. Moreover, PTES will require large thermal storage vessels. As PTES appears to be a very interesting option for long-term energy storage, further development and demonstration projects will be required to accelerate the development of this technology.

Electro-chemical storage plays a secondary role in this analysis, as only cost is considered for large-scale energy storage. Batteries may be preferred as an off-the-shelf solution for smaller applications for shorter time scales or if space is a concern. Economically, Li-ion batteries perform best; however, it is worth looking into alternative batteries, as they perform better in terms of sustainability, recyclability, and fire risk. Furthermore, significant innovation is taking place in the development of batteries, leading to better performance than assumed in this paper.

Flexible utilization of CCGT can act as a transition technology by running on natural gas initially and switching to hydrogen in the future to provide carbon-free dispatchable power.

Author Contributions: Conceptualization, S.M. and S.K.; methodology, S.M. and S.K.; software, S.M. and S.K.; validation, S.M. and S.K.; formal analysis, S.M. and S.K.; investigation, S.M. and S.K.; resources, S.M. and S.K.; data curation, S.M. and S.K.; writing—original draft preparation, S.M.; writing—review and editing, S.M. and S.K.; visualization, S.M. and S.K.; supervision, S.K.; project administration, S.K. All authors have read and agreed to the published version of the manuscript.

Funding: This research received no external funding.

Data Availability Statement: Data are available in a publicly accessible repository that does not issue DOIs. Publicly available datasets were analyzed in this study. These data can be found here: https://github.com/ComputerBas/Techno-Economic-Comparison-of-Electricity-Storage-Options-in-a-Fully-Renewable-Energy-System-Repo/tree/main (accessed on 23 February 2024).

Conflicts of Interest: The authors declare that they have no known competing financial interests or personal relationships that could have appeared to influence the work reported in this paper.

References

1. Guarnieri, M.; Liserre, M.; Sauter, T.; Hung, J.Y. Future energy systems: Integrating renewable energy sources into the smart power grid through industrial electronics. *IEEE Ind. Electron. Mag.* **2010**, *4*, 18–37. [CrossRef]
2. Ipakchi, A.; Albuyeh, F. Grid of the future. *IEEE Power Energy Mag.* **2009**, *7*, 52–62. [CrossRef]
3. Bhatnagar, D.; Currier, A.; Hernandez, J.; Ma, O.; Kirby, B. Market and Policy Barriers to Energy Storage Deployment: A Study for the Energy Storage Systems Program. 2013. Available online: https://www.sandia.gov/ess-ssl/publications/SAND2013-7606.pdf (accessed on 23 February 2024).
4. Jülch, V. Comparison of electricity storage options using levelized cost of storage (LCOS) method. *Appl. Energy* **2016**, *183*, 1594–1606. [CrossRef]
5. Schmidt, O.; Melchior, S.; Hawkes, A.; Staffell, I. Projecting the Future Levelized Cost of Electricity Storage Technologies. *Joule* **2019**, *3*, 81–100. [CrossRef]
6. Steckel, T.; Kendall, A.; Ambrose, H. Applying levelized cost of storage methodology to utility-scale second-life lithium-ion battery energy storage systems. *Appl. Energy* **2021**, *300*, 117309. [CrossRef]

7. IEA. *ETP Clean Energy Technology Guide*; IEA: Paris, France, 2022.
8. IEA. *Grid-Scale Storage*; IEA: Paris, France, 2022.
9. Vistra. Morro Bay Energy Storage Project February 2021. 2021. Available online: https://www.morrobayca.gov/DocumentCenter/View/15093/Vistra---Morro-Bay---Battery-Project-Presentation-022021 (accessed on 21 September 2023).
10. Cole, W.J.; Marcy, C.; Krishnan, V.K.; Margolis, R. Utility-scale lithium-ion storage cost projections for use in capacity expansion models. In Proceedings of the 2016 IEEE North American Power Symposium (NAPS), Denver, CO, USA, 18–20 September 2016; pp. 1–6. [CrossRef]
11. Choi, D.; Shamim, N.; Crawford, A.; Huang, Q.; Vartanian, C.K.; Viswanathan, V.V.; Paiss, M.D.; Alam, M.J.E.; Reed, D.M.; Sprenkle, V.L. Li-ion battery technology for grid application. *J. Power Sources* **2021**, *511*, 230419. [CrossRef]
12. Nitta, N.; Wu, F.; Lee, J.T.; Yushin, G. Li-ion battery materials: Present and future. *Mater. Today* **2015**, *18*, 252–264. [CrossRef]
13. Zakeri, B.; Syri, S. Electrical energy storage systems: A comparative life cycle cost analysis. *Renew. Sustain. Energy Rev.* **2015**, *42*, 569–596. [CrossRef]
14. Kumar, D.; Rajouria, S.K.; Kuhar, S.B.; Kanchan, D.K. Progress and prospects of sodium-sulfur batteries: A review. *Solid State Ion.* **2017**, *312*, 8–16. [CrossRef]
15. McKeon, B.B.; Furukawa, J.; Fenstermacher, S. Advanced lead-acid batteries and the development of grid-scale energy storage systems. *Proc. IEEE* **2014**, *102*, 951–963. [CrossRef]
16. Ding, C.; Zhang, H.; Li, X.; Liu, T.; Xing, F. Vanadium flow battery for energy storage: Prospects and challenges. *J. Phys. Chem. Lett.* **2013**, *4*, 1281–1294. [CrossRef]
17. Zhang, H.; Lu, W.; Li, X. Progress and Perspectives of Flow Battery Technologies. *Electrochem. Energy Rev.* **2019**, *2*, 492–506. [CrossRef]
18. Yong, Q.; Tian, Y.; Qian, X.; Li, X. Retrofitting coal-fired power plants for grid energy storage by coupling with thermal energy storage. *Appl. Therm. Eng.* **2022**, *215*, 119048. [CrossRef]
19. Novotny, V.; Basta, V.; Smola, P.; Spale, J. Review of Carnot Battery Technology Commercial Development. *Energies* **2022**, *15*, 647. [CrossRef]
20. Banaszkiewicz, M. Steam turbines start-ups. *Trans. Inst. Fluid-Flow Mach.* **2014**, *126*, 169–198.
21. Cherif, S. Potential for Power-to-Heat in the Netherlands 3.E04.1-Potential for Power-to-Heat in the Netherlands. 2015. Available online: https://cedelft.eu/wp-content/uploads/sites/2/2021/04/CE_Delft_3E04_Potential_for_P2H_in_Netherlands_DEF.pdf (accessed on 23 February 2024).
22. Laughlin, R.B. Pumped thermal grid storage with heat exchange. *J. Renew. Sustain. Energy* **2017**, *9*, 044103. [CrossRef]
23. Smallbone, A.; Jülch, V.; Wardle, R.; Roskilly, A.P. Levelised Cost of Storage for Pumped Heat Energy Storage in comparison with other energy storage technologies. *Energy Convers. Manag.* **2017**, *152*, 221–228. [CrossRef]
24. Rehman, S.; Al-Hadhrami, L.M.; Alam, M.M. Pumped hydro energy storage system: A technological review. *Renew. Sustain. Energy Rev.* **2015**, *44*, 586–598. [CrossRef]
25. Zhou, Q.; Du, D.; Lu, C.; He, Q.; Liu, W. A review of thermal energy storage in compressed air energy storage system. *Energy* **2019**, *188*, 115993. [CrossRef]
26. California Energy Commision. *Pecho Energy Storage Center*; California Energy Commision: Sacramento, CA, USA, 2021.
27. Mongird, K.; Viswanathan, V.V.; Balducci, P.J.; Alam, M.J.E.; Fotedar, V.; Koritarov, V.S.; Hadjerioua, B. Energy Storage Technology and Cost Characterization Report. 2019. Available online: https://energystorage.pnnl.gov/pdf/PNNL-28866.pdf (accessed on 23 February 2024).
28. Barbour, E. Thermodynamics of CAES. Energy Systems and Energy Storage Lab. 2014. Available online: http://www.eseslab.com/posts/blogPost_CAES_thermodynamics (accessed on 23 February 2024).
29. Kim, J.; Noh, Y.; Chang, D. Storage system for distributed-energy generation using liquid air combined with liquefied natural gas. *Appl. Energy* **2018**, *212*, 1417–1432. [CrossRef]
30. Guizzi, G.L.; Manno, M.; Tolomei, L.M.; Vitali, R.M. Thermodynamic analysis of a liquid air energy storage system. *Energy* **2015**, *93*, 1639–1647. [CrossRef]
31. Vecchi, A.; Li, Y.; Ding, Y.; Mancarella, P.; Sciacovelli, A. Liquid air energy storage (LAES): A review on technology state-of-the-art, integration pathways and future perspectives. *Adv. Appl. Energy* **2021**, *3*, 100047. [CrossRef]
32. Mongird, K.; Viswanathan, V.; Alam, J.; Vartanian, C.; Sprenkle, V.; Baxter, R. 2020 Grid Energy Storage Technology Cost and Performance Assessment. *Energy* **2020**, 6–15. Available online: https://www.pnnl.gov/sites/default/files/media/file/Final%20-%20ESGC%20Cost%20Performance%20Report%2012-11-2020.pdf (accessed on 23 February 2024).
33. Bouten, T.; Withag, J.; Axelsson, L.-U.; Koomen, J.; Jansen, D.; Stuttaford, P. Development and Atmospheric Testing of a High Hydrogen FlameSheetTM Combustor for the OP16 Gas Turbine. In *Volume 3A: Combustion, Fuels, and Emissions*; American Society of Mechanical Engineers: New York, NY, USA, 2021. [CrossRef]
34. Lazard. Levelized Cost of Energy+. 2023. Available online: https://www.lazard.com/research-insights/levelized-cost-of-energyplus/ (accessed on 23 February 2024).
35. Schoenfisch, M.; Dasgupta, A. Grid-Scale Energy Storage. 2022. Available online: https://www.iea.org/energy-system/electricity/grid-scale-storage (accessed on 23 February 2024).
36. Frauenhofer ISE. Monthly Electricity Spot Market Prices in Germany in September 2023. Available online: https://energy-charts.info/charts/price_average/chart.htm?chartColumnSorting=default (accessed on 24 September 2023).

37. ENTSO-E. ENTSO-E Transparancy Platform. 2020. Available online: https://transparency.entsoe.eu// (accessed on 15 November 2023).
38. Hirth, L.; Mühlenpfordt, J.; Bulkeley, M. The ENTSO-E Transparency Platform—A review of Europe's most ambitious electricity data platform. *Appl. Energy* **2018**, *225*, 1054–1067. [CrossRef]
39. Bernath, C.; Deac, G.; Sensfuß, F. Impact of sector coupling on the market value of renewable energies—A model-based scenario analysis. *Appl. Energy* **2021**, *281*, 115985. [CrossRef]
40. Bogdanov, D.; Ram, M.; Aghahosseini, A.; Gulagi, A.; Oyewo, A.S.; Child, M.; Caldera, U.; Sadovskaia, K.; Farfan, J.; Barbosa, L.D.S.N.S.; et al. Low-cost renewable electricity as the key driver of the global energy transition towards sustainability. *Energy* **2021**, *227*, 120467. [CrossRef]
41. Schmidt, O. System Integration of Low-Carbon Electricity. 2023. Available online: https://www.storage-lab.com/emission-mitigation (accessed on 21 September 2023).
42. Heide, D.; von Bremen, L.; Greiner, M.; Hoffmann, C.; Speckmann, M.; Bofinger, S. Seasonal optimal mix of wind and solar power in a future, highly renewable Europe. *Renew. Energy* **2010**, *35*, 2483–2489. [CrossRef]
43. Sens, L.; Neuling, U.; Kaltschmitt, M. Capital expenditure and levelized cost of electricity of photovoltaic plants and wind turbines—Development by 2050. *Renew Energy* **2022**, *185*, 525–537. [CrossRef]
44. Heffron, R.; Körner, M.F.; Wagner, J.; Weibelzahl, M.; Fridgen, G. Industrial demand-side flexibility: A key element of a just energy transition and industrial development. *Appl. Energy* **2020**, *269*, 115026. [CrossRef]
45. Zhang, L.; Sun, C.; Cai, G.; Koh, L.H. Charging and discharging optimization strategy for electric vehicles considering elasticity demand response. *eTransportation* **2023**, *18*, 100262. [CrossRef]
46. Cole, W.; Karmakar, A. *Cost Projections for Utility-Scale Battery Storage: 2023 Update*; NREL: Golden, CO, USA, 2023.
47. Schmidt, O.; Staffel, I. *Monetizing Energy Storage*, 1st ed.; Oxford University Press: Oxford, UK, 2023.